**February 2023**

**Ph. D. Dissertation**

# Clinical and genetic analysis of severe fever with thrombocytopenia syndrome in Korea

**Graduate School of Chosun University**

**Department of Biomedical Sciences**

**Shilpa Chatterjee**

# Clinical and genetic analysis of severe fever with thrombocytopenia syndrome in Korea

국내 중증열성혈소판감소증의 임상 및 유전학적 분석

**February 24th 2023**

**Graduate School of Chosun University**

**Department of Biomedical Sciences**

**Shilpa Chatterjee**

# Clinical and genetic analysis of severe fever with thrombocytopenia syndrome in Korea

**Advisor: Professor. Dong-Min Kim, MD, Ph.D.**

*This Dissertation Submitted to the Graduate School of Chosun University*

*in Partial Fulfillment of the Requirements for*

*The Degree of Doctor of Philosophy in Biomedical Sciences*

**October 2022**

**Graduate School of Chosun University**

**Department of Biomedical Sciences**

**Shilpa Chatterjee**

**This is to certify that the Ph.D. dissertation of Shilpa Chatterjee has successfully met the dissertation requirement of Chosun University**

| | |
|---|---|
| Committee Chairperson, Chosun University | Prof. Cheol-Hee Choi (Sign) |
| Committee Member, Chosun University | Prof. Dong-Min Kim (Sign) |
| Committee Member, Chosun University | Prof. Choon-Mee Kim (Sign) |
| Committee Member, Chosun University | Prof. Sung-Chul Lim (Sign) |
| Committee Member, Seoul National University | Prof. Nam-Hyuk Cho (Sign) |

**January 2023**

# Graduate School of Chosun University

# CONTENTS

# LIST OF TABLES

# LIST OF FIGURES

# 초 록 (ABSTRACT)

## 국내 중증열성혈소판감소증의 임상 및 유전학적 분석

챠테르지 쉴파
지도교수: 김동민 교수
의과학과
조선대학교 대학원

**배경:** 중증열성혈소판감소증후군(SFTS)은 진드기를 매개체로 하는 질병으로서, Phenuiviridae family 의 *Banyangvirus* genus 에 새롭게 추가된 SFTS 바이러스(SFTSV)에 의해 발생하는 감염성 동물원증이다. SFTS 는 발열, 혈소판 감소, 백혈구 감소가 주요 특징이며, 동아시아 국가에서 SFTS 환자의 수는 매년 증가하고 있다. 국내 SFTS 환자의 평균 발생율은 지역별 및 연도별로 차이가 있음에도 불구하고 SFTS 환자의 치사율은 6% ~ 21%로 일본, 한국, 중국에서 상당히 높게 나타난다. SFTS 바이러스에 의해 다양한 임상적 증상이 나타나며, 국가 간에 사망률에 차이가 나는 이유는 불분명하다. 또한 임상적

증상에 대한 기준은 아직까지 불명확하다. 임상 및 공중 보건의 중요성에도 불구하고, 현재 SFTS 바이러스에 대해 안전하고 효과적인 임상적 치료제뿐만 아니라 백신 개발이 완료되지 않았다. 이를 해결하기 위해 본 연구에서는 한국인 집단에서 SFTS 바이러스의 분자적 평가, 유전적 특성, 동시감염 및 SFTS 에 대한 치료적 방법을 조사하고자 하였다.

**방법:** 다기관 SFTS 임상 코호트 연구를 수립하여, 국내 대학병원별 SFTS 환자의 역학적, 임상적 특성을 분석하기 위해 후향연구를 수행하였다. 본 연구는 2015 년부터 2022 년까지 총 129 명의 환자를 대상으로 진행되었다. SFTS 의 진단은 SFTS 환자의 혈액 속 SFTS 바이러스 RNA 를 검출하는 nested PCR 결과를 기반으로 이루어졌다. PCR 결과를 통하여 SFTS 양성 환자는 역학적 자료, 임상적 특징, 치료 결과 및 실험 결과를 토대로 자료를 수집하였다. SFTS 이외의 다른 병원체의 감염여부와 동시감염을 확인하기 위해 multiplex 및 singleplex real-time PCR 분석을 수행하였다. 또한 임상 검체의 유형별 항원 검출을 위해 nested PCR 분석을 수행하여 *Orientia tsutsugamushi* 및 *rickettsia* 를 검출하였다. SFTS 바이러스의 변종을 식별하기 위해 Sanger sequencing 분석을 수행하였다. 서로 다른 종들 사이의 진화적 관계를 확인하기 위해 계통발생학적 분석이 수행되었다. 또한 잠재적으로 SFTS 바이러스에 효과적인 약물을 개발하기 위해 SFTS 단백질을 대상으로 *in silico* 약물의 용도 변경 연구를 수행하고 SFTS 바이러스에

대한 해당 분자의 항바이러스 활성을 추가로 측정하기 위해 플라크 분석을 수행하였다.

**결과:** SFTS 양성 사례 129 건 중 환자의 대다수는 50 세 이상으로 치사율이 19.4%에 달했다. 전라도는 가장 많은 환자가 발생한 지역이며, SFTS 감염이 가장 많이 발생하는 계절은 봄과 여름인 것으로 나타났다. 또한 고령환자(70 세)의 사망률이 가장 높았으며 감염환자의 연령대별 사망률에서도 유의한 차이를 보였다. SFTS 바이러스 L, M, S segment 유전자 및 계통발생학적 분석 결과 한국의 SFTS 바이러스는 A-F 유전형으로 분류할 수 있으며, B 유전형의 세분화된 유전형인 B-1, B-2, B-3 중에 B-3 유전형의 SFTS 바이러스가 치사율 17.4%로서 가장 널리 퍼져 있다. 또한 B-1 유전형의 SFTS 바이러스가 23.8%로 가장 높은 치사율을 보였다. 또한, 우리는 한국의 SFTS 바이러스 균주가 L, M, S segment 간의 역동적인 재분류(reassortment)를 통해 새로운 유전형의 바이러스로 진화할 수 있으며, 단일 SFTS 균주에서 segment 간에 서로 다른 유전형의 존재를 확인하였다. 또한 SFTS 환자 중 1.6%(95% CI, 0.001 – 0.06)는 *O. tsutsugamushi* 56 kDa 유전자를 타겟으로한 nested PCR 양성으로 쯔쯔가무시병과 중복감염을 보였으며, SFTS 환자 중 6.2%(95% CI, 0.03–0.13)는 *rickettsia* spp.

*ompA* 유전자를 타겟으로한 nested PCR 양성으로 리케차증과 중복감염을 나타냈다. *O. tsutsugamushi* 56 kDa 유전자를 대상으로 한 계통수 분석 결과, 본 연구에서 발견된 Boryong 균주는 서울시에 발견된 다른 *O. tsutsugamushi* 균주와 밀접하게 군집해 있었다. 또한 *rompA* 유전자를 대상으로한 계통발생학적 분석은 본 연구에서 발견된 7 개의 서열이 *rickettsia monacensis* 와 밀접하게 군집되어 있고 1 개의 서열이 *rickettsia tamurae* 균주와 군집을 형성하고 있음을 보여주었다. 또한 SFTSV L 단백질을 대상으로 한 *in silico* 분석은 SFTS 바이러스에 효과가 있는 4 개의 잠재적인 약물을 확인하였다. 항바이러스 분석은 $EC_{50}$ 값이 100-200 μg/mL 범위에 있음을 밝혀냈으며, 이는 모든 화합물이 약한 항바이러스 활성을 지녔음을 나타낸다.

**결론:** 전반적으로 SFTS 바이러스에 대한 유전·역학 연구는 한국에서 SFTS 바이러스의 유전체 변이와 병인에 대한 이해를 향상시킬수 있다. 환자들의 임상 데이터에 대한 조사는 질병 진행 및 사망률 측면에서 나이가 중요한 요소라는 것을 밝혀냈다. SFTS 바이러스는 새로운 유전형을 생성하여 진단을 더욱 어렵게 하였다. 또한, 우리의 연구 결과는 SFTS 와 쯔쯔가무시병 및 리케차증과 같은 다른 감염병의 동시 감염을 밝혀냈으며, 이는 이러한 질병이 자연적으로 풍토병인 지역에서 동시 감염이 제거될 때까지 독시사이클린 치료가 필요할 수 있음을 시사한다. 비록 이 연구에서 효과적인 치료 방법이 확인되지는 않았지만,

우리는 연구가 SFTS 의 연구에 대한 관심을 증가시키고 SFTS 바이러스의 유전 구조와 진화에 대한 보다 나은 이해에 기여하기를 희망한다. 게다가 SFTS 바이러스 유전체와 SFTS 전파에 대한 지속적인 모니터링 및 심층연구는 SFTS 의 심각한 발병을 예방하는 데 필요하다.

# ABSTRACT

## Clinical and genetic analysis of severe fever with thrombocytopenia syndrome in Korea

Shilpa Chatterjee
Advisor: Prof. Dong-Min Kim
Department of Biomedical Sciences
Graduate School of Chosun University

**Background:** Severe fever with thrombocytopenia syndrome (SFTS) is an infectious zoonosis which is caused by the SFTS virus (SFTSV). SFTS comes under the genus of *Phlebovirus,* family *Bunyaviridae*. The primary clinical manifestations of SFTS are fever, leukopenia, and thrombocytopenia. Each year increasing number of SFTS patients has been observed having fatality rate ranges between 6% to 21% which primarily affects China, South Korea, and Japan. The mean SFTS case mortality rate has stayed fairly high in China, South Korea, and Japan, despite regional and annual variations. The mechanisms underlying the various clinical presentations induced by this virus and the reasons why fatality rates vary between nations are mainly unclear; nevertheless, underlying medical conditions are suspected. Moreover, despite its clinical and public

health importance, there are currently no clinical, pharmaceutical, or vaccination treatments that are both safe and effective. To address this, here I aimed to perform the molecular evaluation and genetic characteristics of SFTSV in South Korean population, frequency of coinfection and probable therapeutic options for SFTS.

**Methods:** A multicenter clinical cohort study of SFTS was conducted. In order to examine the epidemiological and clinical traits of patients with SFTS in several university hospitals in Korea, retrospective studies were carried out. A total of 129 patients from 2015 to 2022 were enrolled for this study. Based on the findings of a nested polymerase chain reaction (PCR) to find viral RNA in the blood of SFTS patients, the condition was diagnosed as SFTS. After evaluating medical records, epidemiologic information, clinical characteristics, laboratory findings, and treatment outcomes of patients with SFTS were obtained. In order to identify the presence of any other pathogen, I investigated the frequency of coinfection in all patients by performing multiplex and single design q-PCR assay. Further, nested PCR assays were performed for the type-specific antigen detection from clinical samples to detect *Orientia tsutsugamushi* and spotted fever group *rickettsia* species. Sanger sequencing analysis was performed to identify the species strain. Phylogenetic analysis was performed to confirm the evolutionary relationship among different species. Additionally, in-silico drug repurposing study was performed targeting SFTS protein to identify potential lead

molecule and in-vitro plaque assay was performed to further measure the antiviral activity of those molecules against SFTSV.

**Results:** Among 129 SFTS positive cases, majority were about 50 years old with 19.4% fatality rate. Jeolla province was identified to be the most prevalent area with the greatest number of cases and Summer and Autumn were the most prevalent season for SFTS infection. Also, elderly patients aged ≥70 years displayed the highest fatality rate and there was a significant difference in the fatality rate between different age group of infected patients. Genetic and phylogenetic analysis showed that Korean SFTSV can be distinguished into genotype A-F with B-3 being the most prevalent genotype with fatality rate of 17.4%. Genotype B-1 showed the highest fatality rate of 23.8%. Further, I identified the presence of different reassortants in a single strain which indicates that the Korean strains of SFTSV were dynamically evolving through active reassortments that resulted in a diversity of novel genotypes. Additionally, the frequency of coinfection of SFTS with other zoonoses was ruled out which revealed 1.6% (95% CI, 0.001–0.06) scrub typhus positive patients and 6.2% (95% CI, 0.03–0.13) rickettsiosis positive coinfected patients. Phylogenetic tree analysis targeting 56 kDa gene showed that the strain Boryong found in our study were closely clustered with other *O. tsutsugamushi* strain isolated in Seoul city, Korea. Further, phylogenetic tree analysis targeting *rompA* gene showed that 7 sequences found in our study were closely clustered with *Rickettsia monacensis* and 1 sequence formed cluster with *Rickettsia tamurae* strain. Additionally,

in-silico analysis targeting SFTSV-L protein identified four possible lead molecules against SFTSV. Antiviral assay revealed that the $EC_{50}$ values in the range between 100-200µg/mL which indicates that all the compounds are less potent owing to very weak antiviral activity.

**Conclusions:** Overall, the genetic and epidemiological research on SFTSV enhances our understanding of the SFTS's pathogenic and genomic variation in South Korea. Investigation on patients' clinical data revealed that age is an important factor in terms of disease progression and mortality. Also, the dynamic evolutionary nature of SFTSV strains were understood, leading to the generation of new genotypes and making diagnosis more difficult. Additionally, our study findings revealed the frequency of coinfection of SFTS with other zoonoses which suggests that the regions where these diseases are endemic in nature, doxycycline treatment may be necessary until coinfection is eliminated. Although, no effective therapeutic options were identified in this study still I am hopeful that our research will increase interest in the study of SFTS and contribute to a deeper knowledge of the genetic structure and evolution of SFTSV. Moreover, continuous monitoring studies and in-depth research into the SFTSV genome and SFTS propagation are required to help prevent severe outbreaks of SFTS.

# I. INTRODUCTION

## 1.1. Background

Severe fever with thrombocytopenia syndrome (SFTS) is a newly found zoonoses which is caused by the virus *Dabie bandavirus* or another name SFTS virus (SFTSV). SFTSV comes under *Bunyaviridae* family, genus *Phlebovirus* [1]. Mainly SFTSV spreads by several tick species; among which *Haemophysalis longicornis* is the pivotal one. Several other cases of tick-borne SFTSV were also reported such as, *Rhipicephalus microplus, Ixodes nipponensis,* and *Amblyomma testudinarium.* Patient with SFTS shows primary signs of high fever, diarrhea, thrombocytopenia, gastrointestinal symptoms, and leukopenia [1-3]. SFTSV is an RNA virus which is negative stranded and genome consists of three segments names (L), medium (M), and small (S) with a total diameter size of 80–120 nm [2] (**Figure 1**). The viral RNA-dependent RNA polymerase (RdRp), which initiates viral RNA replication and transcription, is expressed by the L segment and contains its 6368 amino acids. The 3378 amino acids that make up the precursor to the glycoproteins Gn and Gc, which are in charge of creating viral particles and causing them to adhere to target cells, are encoded by the M segment. Lastly, the S segment uses ambisense transcription to encode the nucleocapsid protein (N) as well as a nonstructural protein (NSs) [4].

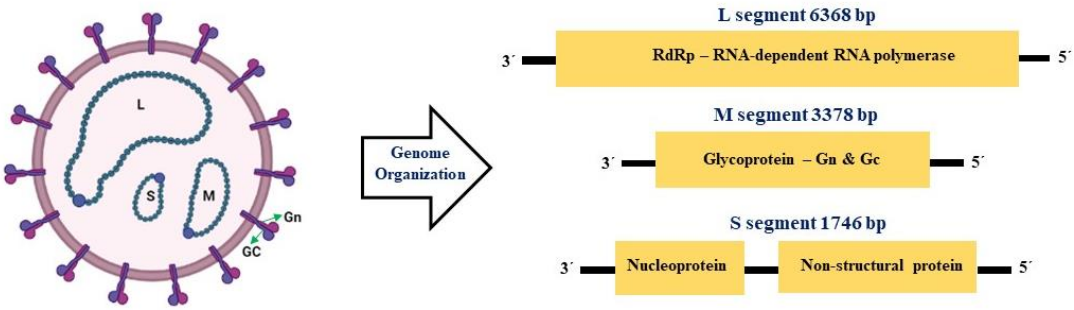


**Figure 1. Schematic diagram of SFTSV**

SFTSVs can be divided into 6 genotypes (A-F) based on phylogenetic study [5]. SFTSV can be spread to human by infected tick bite [2,6]. In the year 2009, the country China reported the first SFTS case and after that, South Korea and Japan also reported the SFTS cases [7,8]. Since then, several cases have been found and South Korea reported 1696 SFTS cases with 277 reported death between 2013 to 2022 [9]. SFTS patients are mainly found in East Asian countries having 16.4% mean death rate [7]. On the basis of increasing case-fatality rate (CFR) and propensity for epidemic propagation of SFTS, the World Health Organization listed SFTS as among the 10 leading infectious diseases that need immediate attention [10].

## 1.2. Clinical manifestations and characteristics of SFTS

Depending on viral loads and the point of infection, the incubation period for SFTS can be anywhere between 5 and 14 days [11]. Fever, gastric symptoms including nausea, vomiting, stomach ache, and diarrhea, as well as neurological symptoms such mental state changes are the most common symptoms that patients report [2,11]. Flu-like symptoms, such as sudden fever, weakness, muscle pain, lymphadenopathy, disorientation, and sickness, are typically seen during the early fever stage. Anorexia, nausea, vomiting, and diarrhea are gastrointestinal signs. Additionally, present are respiratory symptoms such expectoration and coughing [3,11]. Critical stage complications include severe bleeding, neurological problems, acute respiratory symptoms, and cystic fibrosis, which can result in sepsis, disseminated intravascular coagulation, and other potentially fatal conditions [12]. Patients with SFTS typically have bleeding. Hematemesis, melena, ecchymosis, gingival bleeding, hemoptysis, ophthalmorrhagia, and petechia were among the more severe hemorrhagic signs that 35.07% of SFTSV infected patients had, according to prospective observational research [13]. SFTSV may therefore be characterized like a hemorrhagic fever virus. In the later phase, disease progress with cytokine storm and hemophagocytic lymphohistiocytosis that makes the process more complicated.

## 1.3. Disease progression and diagnosis of SFTS

SFTS is challenging to diagnose for clinicians if the individual is unaware of it. Patients frequently have symptoms like fever, reduced platelet and WBC counts. Patients with tick bite history should be considered as cases of SFTS, mainly in the SFTSV endemic places. For the survival of the patients, it is challenging to overstate the significance of an early detection of SFTSV. The lack of specificity in the clinical signs of SFTS necessitates laboratory confirmation; also, other tick-borne diseases produce similar symptoms [14,15]. Reverse transcriptase (RT) real-time PCR can be very specific and sensitive approach to detect SFTSV viral RNA [16]. Moreover, Yoshikawa et al. developed a QRT-PCR that may identify genetically distinct SFTSV strains [17]. Additionally, several PCR strategies are now being created to more quickly and easily detect SFTSV. Reverse transcription-loop-mediated isothermal amplification (RT-LAMP), developed by Huang et al., offers 100% specificity and 99% sensitivity for finding new bunyaviruses [18]. Additionally, Baek et al. showed that RT-LAMP has a higher sensitivity than general RT-PCR and can provide a diagnosis in 30 to 60 minutes [19]. For detecting antibody such as SFTS specific IgM and IgG in the serum one-week post illness, IFA or an ELISA are reliable diagnostic techniques [20]. However, in the early stages of SFTS, IFA or ELISA may not be sufficient [20]. Clinical symptoms and test outcomes of patients with these diseases are similar to those with SFTS [21]. Therefore, alternative diagnosis is crucial in places wherein SFTS coexist with other zoonoses.

## 1.4. SFTS epidemiology, transmission, pathogenesis, and prevention

Tick-borne zoonotic infection is the primary source of SFTSV infection. Livestock, non-domesticated animals, and ticks are all potential hosts for SFTSV [11,22]. The thorough investigation found that 24% of SFTS patients had been infected by ticks [23]. As a result, factors that encourage tick growth and reproduction, frequent outdoor human activity, and increased tick or animal contact are all potential risk factors for SFTSV infection. 6 Asian countries have reported verified number of cases of SFTSV since it was first isolated in 2010 [24-29].

Between April and November, individuals typically become unwell. In addition to the three prominent East Asian nations, patients with SFTS have recently been found in Southeast Asia [27,30–31]. Further, animal SFTSV was also reported [30]. Cases similar to SFTS were also United States [32,33]. *H. longicornis* like several other tick species are involve in SFTSV transmission [1,34,35]. The *H. longicornis* is the pivotal vector of SFTSV which can be found in endemic temperate areas [36]. A study informed that the patient having SFTS encephalopathy and the *H. longicornis* tick that bit her were found to have the same SFTSV [37]. Another report stated that this tick prevalence is higher in endemic regions than other areas which again proved its dominance as SFTSV vector [37]. Additionally, Zhuang et al. stated the SFTSV RNA transmission in the reproductive system of infected ticks after microinjecting SFTSV into *H. longicornis* [38].

Although the pathophysiology of SFTS is not entirely known, it is associated with an increased viral load and inflammatory responses induced by several cytokines, including granulocyte colony stimulating factor (GCSF), interleukin 1, 6, and 10 receptor antagonist and many other [39-40]. Below is the diagram of SFTSV pathogenesis (**Figure 2**).

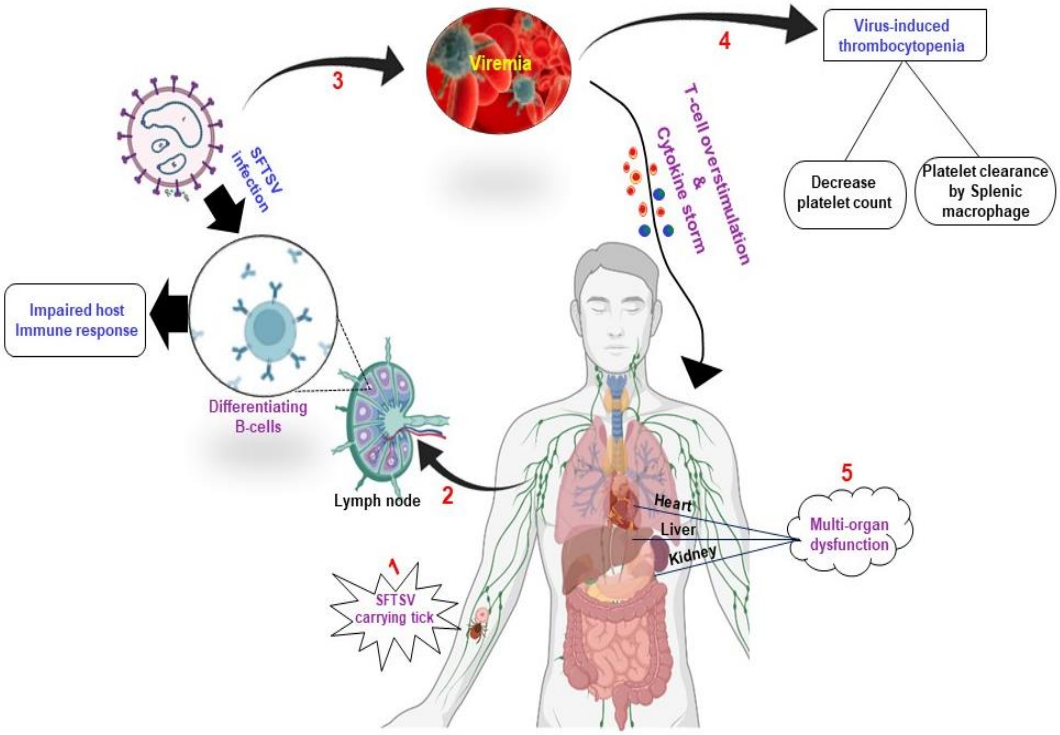

**Figure 2. Pathogenesis of severe fever with thrombocytopenia syndrome virus**

**1 -** SFTSV human transmission via tick-bite. **2 –** SFTSV carrying tick target nearest lymph nodes generating impaired immune response via B-cell differentiation. **3 –** Further replication of SFTSV into systemic circulation and occurrence of viremia causing cytokine storm and T-cell overstimulation. **4 –** viremia induced thrombocytopenia; causing reduced platelet count and virus bound platelet sequestration by splenic macrophages. **5 –** endothelial damages and compromised immune system cause multi-organ damages (Created with BioRender.com).

There are currently no commercially available chemoprophylactic drugs or vaccines for the treatment of SFTS. Numerous papers have speculated on potential treatments, but none have proven successful for ongoing use [41]. Avoiding tick bites is the main preventative measure in endemic areas. Bedding and garments should be thoroughly shaking and laundered after outside activities. Other efficient prevention strategies include bathing or showering right away after being outside, looking for tick bites, then getting rid of ticks as soon as feasible. Additionally, in locations where the disease is endemic, it is best to avoid direct contact with domestic animals' bodily fluids (such as cats or dogs) [42,43]. Although standard safety measures are advised for SFTS patients, it is possible for SFTSV to spread through several paths in patients who have severe SFTS since it is challenging to pinpoint the exact transmission route. Therefore, active caution is needed, such as isolation [44].

These findings underline the urgent need for epidemiologic research on vector-borne infections in areas of endemicity in order to enhance our capacity to distinguish febrile infectious diseases with atypical first signs and symptoms and rapidly treat them. Therefore, considering the severity of the disease and the lack of its effective prevention, I aimed to examined the epidemiological and clinical characteristics of suspected SFTS patients in South Korea. Further, I investigated the genotypic diversity of the SFTSV and performed the molecular investigation to identify the frequency of coinfection of SFTS with other zoonoses. Along with that, I aimed to identify the probable therapeutic options against SFTSV.

# II. OBJECTIVE AND SCOPE

SFTS is a newly detected viral hemorrhagic fever disease which mainly spread by ticks. The pivotal symptoms of SFTS are fever, thrombocytopenia, gastrointestinal symptoms, and leukopenia and can be contagious. Since its first discovery in 2011, many cases have been reported in southeast Asian countries and also in India, US with 16.4% mortality rate. In South Korea, each year rising number of patients (231 fatal cases) have been reported mainly in the tick-bite season of Summer and Autumn. SFTSV undergoes dynamic genomic mutations that resulted in a formation of new genotype, make it difficult to diagnose. Not only ticks, SFTSV cases of non-vector transmission has also been identified. Further, SFTS disease also share comparable risk factors and overlapping geographical distribution with other zoonoses which is an actual clinical concern in relation to laboratory diagnosis and treatment.

However, considering the severity of SFTS, presently, no safe and effective clinical, pharmacological and vaccine options are present for SFTS. This creates the necessity for the identification of quality detection and diagnosis method, epidemiological study, investigation of genotypic diversity, and probable treatment options. To address this, in this research I aimed to analyze the prevalence of SFTS in South Korean population by focusing on its detection, diagnosis, epidemiology, genotypic diversity, frequency of coinfection and probable treatment option against SFTSV. The prime objective of the

current study is to perform a clinical and molecular investigation targeting the clinical population affected with SFTS and focusing on disease detection, epidemiology, diagnosis, genotypic diversity, incidence of coinfection and effective treatment strategies against SFTSV.

# III. MATERIALS AND METHODS

## 3.1. Participants and data source

I performed a multicenter clinical cohort study where the confirmed SFTS cases were selected based on following criteria: identification of SFTSV RNA by using at least 2 or more nested PCRs targeting M segment and S segment.

Among 382 suspected cases, 129 SFTS positive patients from 14 institutions were enrolled in the study. Institutional Review Board from all the institution were approved and patients provided the consent to perform the study. The inclusion criteria: 1) patients whose age 19 years and older with SFTS and admitted to hospitals from 2015 to mid of 2022, and 2) those who confirmed SFTS by molecular test for SFTSV. Patients with invalid clinical data were excluded from the study.

## 3.2. Nucleic acid extraction and complementary DNA (cDNA) synthesis

The SFTS patients' blood was drawn for sampling. After symptom onset to sample collection was average 5.1 days, and the average sample collection date was 11.5 days. Following the manufacturer's instructions, 300 μL blood samples were used to extract viral RNA using the Viral Gene-spinRNA Extraction Kit (iNtRON Biotechnology in Seongnam, Korea). Before usage, the isolated RNA was kept at -70°C. The SuperScriptVILO MasterMix (Thermo Fisher, San Francisco, CA, USA) was used to

create the cDNA in accordance with the manufacturer's instructions and kept at -20°C until it was needed.

### 3.3. Molecular detection of SFTSV by polymerase chain reaction (PCR)

One-step reverse transcription polymerase chain reaction was used to detect the SFTSV M segment gene as a confirmation test for SFTSV infection (RT-PCR). Using an inner primer [SFTS-F(MF3)/SFTS-R(MF2)] from a previously published report [45], the SFTSV nested PCR targeting the M-segment was carried out, whereas I created the outer primer set SFTS-M 1st-F and SFTS-M 1st-R. A 20 μL sample including 2 μL of cDNA template, 0.5 pmol of particular primers, and the AccuPower Taq PCR PreMix was used to conduct the PCR (Bioneer, Daejeon, Korea). **Table 1** contains information about primers and probes.

**Table 1. Oligonucleotide primer used to perform PCR to detect the molecular target in SFTS virus**

| Target | Primer | Nucleotide sequence (5′–3′) | Fragment length (bp) | Reference |
|---|---|---|---|---|
| M segment | SFTS-M 1st-F | TCATCCTGACYTATTYTGCAATWG | 640 | [45] |
| | SFTS-M 1st-R | TAAGTYACACTCACACCCTTGAA | | |
| | SFTS-F(=MF3) | GATGAGATGGTCCATGCTGATTCTAA | 560 | |
| | SFTS-R(=MR2) | CTCATGGGGTGGAATGTCCTCAC | | |
| S segment | SFTS-S-NP-2F | CATCATTGTCTTTGCCCTGA | 461 | [46] |
| | SFTS-S-NP-2R | AGAAGACAGAGTTCACAGCA | | |
| | SFTS-S-N2F | AAYAAGATCGTCAAGGCATCA | 346 | |
| | SFTS-S-N2R | TAGTCTTGGTGAAGGCATCTT | | |

A 20 μL sample including 2 μL of cDNA template, 0.5 pmol of particular primers, 0.25 pmol of particular probe, and 4 L of the LightCycler TaqMan Master mix was used to conduct the PCR. Exicycler Quantitative Thermal Block (Bioneer, Daejeon, Korea) was used for amplification and detection under the following conditions: 5 minutes of pre-denaturation at 95°C, 45 cycles of 5 second of denaturation at 95°C, and 5 second of primer annealing at 55°C. To measure SFTSV RNA, positive control plasmids were created as a standard. A NanoDrop spectrophotometer was used to measure the plasmid concentration (Thermo Fisher, San Francisco, CA, USA). An online calculator was used to determine the quantity of SFTSV RNA copies (http://cels.uri.edu/gsc/cndna.html,

accessed on 19 April 2022). The positive control plasmids were then utilized in real-time PCR to create a calibration curve after being serially diluted from $10^8$ to $10^1$.

## 3.4. Molecular detection of *Orientia tsutsugamushi* by PCR

A diagnosis of scrub typhus was established if two or more target genes of *O. tsutsugamushi* positive for PCR: 1) a positive real time PCR (Q-PCR) result by detecting the conserved hypothetical protein (tchA) of *O. tsutsugamushi* and 2) a positive nested PCR result detecting 56-kDa antigen of *O. tsutsugamushi* using 300 µL of whole blood and eschar samples. DNA was isolated from patient whole blood or serum samples using a QIAamp DNA Mini kit (QIAGEN). I performed the three-multiplex Q-PCR targeting conserved hypothetical protein (tchA) of *O. tsutsugamushi*, polymorphic multigene (P44) of *Anaplasma phagocytophylum*, and insertion sequence gene (IS1500) of *Leptospira interrogans* to confirm the PCR positivity and rule out the possible coinfection of scrub typhus, anaplasmosis and leptospirosis respectively.

To further confirm the Q-PCR result, nested PCR was performed targeting 56-kDa antigen of *O. tsutsugamushi*. nested PCR was performed to amplify the 56-kDa antigen of *O. tsutsugamushi* using INNOPLEX$^{TM}$ TSUTSU detection kit (iNtRON Biotechnology, Seoul, Korea) in accordance with the manufacturer's instructions [47-48]. Either an eschar- or buffy coat-based polymerase chain reaction was used to confirm scrub typhus (PCR). Using a set of primers (forward: TTT CGA ACG TGT CTT TAA GC; reverse: ACA GAT GCA CTA TTA GGC AA; 1151 bp), PCR was carried out to

target the variable domains I and II of the 56-kDa antigen gene of *O. tsutsugamushi*. The products were sequenced to complement the reference genotypes, as previously described [47-48].

## 3.5. Molecular detection of *Rickettsia species* by PCR

Genomic DNA from clinical samples was amplified using PCR for molecular identification. Genomic DNA samples were submitted to a nested PCR targeting the outer membrane protein A in order to determine the presence of Rickettsia species in patients (ompA). **Table 2** lists the PCR primers and corresponding product sizes. Using AccuPower PCR PreMix, the reactions were conducted in a total volume of 20 µl, consisting of 16 µl distilled water, 1 µl of each primer (10 pmol/ µl), and 2 µl genomic DNA template (Bioneer, Daejeon, ROK). An AB thermal cycler was utilized to conduct the PCR analysis (Applied Biosystems, Foster City, CA, USA). Each pair of PCRs contained a positive control containing R. conorii DNA and a negative control using distilled water instead of template DNA. After being subjected to electrophoresis on a 1.2% agarose gel containing ethidium bromide, the amplified products were examined using an ultraviolet transilluminator system (FAS-III, Toyobo, Osaka, Japan). As a molecular weight marker, a 100-bp ladder (Bioneer Corp, Korea) was employed.

**Table 2. Oligonucleotide primer used to perform PCR to detect the molecular targets in *Rickettsia* species**

| Target | Primer | Nucleotide sequence (5′–3′) | Fragment length |
|---|---|---|---|
| ompA | RR190.70F | ATGGCGAATATTTCTCCAAAAA | 634 bp (first) |
| | RR190.701R | GTTCCGTTAATGGCAGCATCT | |
| | RR190.70F | ATGGCGAATATTTCTCCAAAAA | 535 bp (nested) |
| | RR190.602R | AGTGCAGCATTCGCTCCCCCT | |

## 3.6. Analysis of viral sequences and phylogenetic analysis

Phylogenetic analysis was performed targeting both SFTSV M segment (477 base pair) and S segment (346 base pair) sequences with ClustalX. Neighbour-joining (N-J) method was used to construct phylogenetic tree. Further, to confirm the *O. tsutsugamushi* positive sequences, phylogenetic analysis was performed targeting *O. tsutsugamushi* 56-kDa gene sequences (475 bp) with ClustalX and were constructed using the neighbour-joining (N-J) method was used to construct phylogenetic tree. Moreover, to confirm the rickettsia positive sequences, phylogenetic analysis was performed targeting *rickettsia ompA* gene sequences (380 bp) with ClustalX and neighbour-joining (N-J) method was used to form phylogenetic tree. The evolutionary history of the examined taxa was represented by a bootstrap consensus tree that was inferred from 1,000 replicates.

## 3.7. Statistical analysis

Frequencies and percentages were used to describe the results of categorical variables, while medians and interquartile ranges were used to display the results of continuous variables (IQRs). The Mann-Whitney U-test was used in analyses to compare continuous variables between patient groups with fatal and non-fatal outcomes. Chi-square or Fisher's exact tests were used for analysis of categorical variables. The Wilson approach with a continuity correction was used to get the lower and upper boundaries of the 95% confidence interval (CI) for the prevalence of coinfection. 95% confidence intervals were considered for all calculated *P* values, which were all two-sided. With the help of the software program GraphPad Prism, statistical analyses were carried out (v. 8.0; GraphPad Software Inc., La Jolla, CA, USA).

## 3.8. In-silico analysis of potential hits against SFTSV

This method described here is already published in our previous study [49]. Again, we described here in a brief form.

- **Protein data preparation**

This process is crucial to the in-silico drug design method. The Protein Data Bank was used to retrieve the structure of the SFTSV L protein (PDB; https://www.rcsb.org/search) (PDB ID: 6XYA). The PyMol software was used to remove bonded co-crystalline water molecules from the protein crystal structure [49]. The bound sodium ion (Na+) in this co-crystalline protein structure was also taken out. The co-crystalline ligand MGP, which was isolated and its data recorded separately, was bound to the protein structure. After that, a pdb file containing the co-crystalline ligand, water, and ion-free protein structure was imported into AutoDock tools software [50]. Polar hydrogen and Kollman charges were then included. The protein coordinates were stored in pdbqt file format, and the uniform distribution of charges was considered.

- **Small molecule database preparation**

The present work made use of the DrugBank (https://go.drugbank.com/) and ChemBridge database (https://chembridge.com/), which are a chemical library. Molecules' two-dimensional (2D) chemical structures were downloaded in SDF file format. All 2D chemical structures were converted into 3D structures using the Open Babel software, which was then optimized for structure and energy minimization [51]. The Open Babel program was run using a custom bash script. An MMFF94 force field

included in Open Babel was used to optimize the structure. Each ligand structure was reduced for 10,000 steps using the steepest descent algorithm [52]. The pdbqt file format was then used to store each minimized structure.

- **Molecular docking–guided virtual screening**

The AutoDock Vina software was utilized for this. The molecular-docking-based virtual screening procedure was implemented using an internal bash script [53]. As a receptor grid, a constrained co-crystalline ligand-binding site was considered. An AutoDock Vina configuration file was created using receptor grid X, Y, and Z coordinates of 2.809, 0.512, and 16.668 correspondingly, and grid box dimensions of 20 Å. The exhaustiveness value was set at 8. Ten conformers for each ligand were kept after the docking-based virtual screening was successfully completed. The docking results were visually inspected using the PyMol program. Images were rendered using Maestro-v12.3 visualization software (Schrödinger Release 2020-1; Maestro, Schrödinger, LLC, New York, NY, 2021).

- **Docking validation**

An important stage in molecular-docking-based virtual screening is this confirmation [54]. The databases were searched for the 3D structure of the co-crystalline ligand MGP in the SDF format. This molecule was produced using the method outlined in the previous subsection, and it was then stored in the pdbqt format. Then, using X, Y, and Z grid coordinates of 2.809, 0.512, and 16.668, respectively, and a grid box dimension setting of 20, the produced molecule DB02716 was docked with the target protein. There

were ten docked conformations reported. The native pose (co-crystalline MGP pose) of each docked conformation was superimposed, and the root mean square deviation (RMSD) was calculated. The RMSD calculation pair_fit plugin script for PyMol (https://pymolwiki.org/index.php/Pair_fit) was used for superimposition.

- **MD simulations**

Gromacs 2018.1 software, which is GPU-accelerated, was used to run these simulations [55]. The protein topology was prepared using the Charmm36 force field [56]. The ligand parameterization topology was created using the online server-based SwissParam program [57]. The TIP3P water model was used to solvate each system, producing a 10×10×10 Å cubic box [58]. Each solvated protein-ligand system was neutralized by the addition of a sufficient quantity (0.15 M) of Na+ and Cl- ions. With a maximum of 100,000 steps, the steepest descent algorithm was used to minimize each system, and the force was set to be less than 10.0 kJ/mole. Analysis was done on two-stage equilibration processes. Volume, temperature, and the number of particles were held constant and maintained for 2 ns in the first step, also known as the NVT ensemble step. The second step is the NPT ensemble step with constant temperature and pressure, and the particle numbers were stabilized for 10 ns. Cα atoms were subjected to a 100 ns positional restriction for each step of equilibration.

The solvent molecules were given full freedom to roam about in order to maintain an equilibrium in the solvent. To constrain the system's covalent bonds, the linear constraint solver algorithm was used [59]. With a cut-off of 1.2 nm and a Fourier spacing of 1.2

nm, the particle mesh Ewald method was utilized to study long-range electrostatic interactions [60]. The temperature (300.00 K) of the system was controlled using the V-rescale weak coupling technique. The Parrinello-Rahman approach was used to control the system's total energy, density, and atmospheric pressure [61]. A 100 ns production run without the use of any restraint was followed by a 2 femtosecond (fs) step for each equilibrated system with acceptable geometry, solPyMOL>pair_ft 6xya_entry_00001_conf_02, ccl-min, and Executive RMS: RMS=1.301 (33 to 33 atoms) vent orientation. Two picosecond (ps) intervals were used to record the structural coordinates. After an MDS was successfully completed, water and ions were removed, and then the trajectories were refined using periodic boundary correction (PBC). Numerous characteristics, including RMSD, RMSF, radius of gyration (Rg), solvent-accessible surface area (SASA), and the number of hydrogen bonds (H-bonds) between the ligand and protein, were computed from the improved trajectories [62–65]. The data were plotted using the Grace software (https://plasma-gate.weizmann.ac.il/ Grace) and the VMD software was used to visualize the trajectory and produce the images [66].

- **Binding Energy Calculation**

The well-known MMPBSA method was used to quantitatively assess the ligand-protein binding relationship [67]. The computation of the MMPBSA-based binding energy was carried out using the MMPBSA method for the GROMACS (g_mmpbsa) script program [68]. A few well-known equations are provided below to clarify this program's fundamental operating idea. It is widely known that a protein-ligand complex requires a

system energy that is lower than the sum of the energies of each of its constituent parts to be stable. Suppose the term ΔGbind refers to the binding free energy of a protein-ligand system. Ten, ΔGbind can be expressed as follows,

$$\Delta Gbind = Gcom - (GP + GL) \quad (1)$$

where Gcom stands for free energy of the protein–ligand system. The abbreviations GP and GL, respectively, stand for the free energy of the ligand and unbound protein in a solvent. Now, Eqs. (2a) and (2b), respectively, can be used to express the parts GP and GL separately.

$$GP = (EMMP) - TS + (Gsolv) \quad (2a)$$

$$GL = (EMMP) - TS + (Gsolv) \quad (2b)$$

where temperature and entropy are represented, respectively, by T and S. Gsolv is the free energy of solvation, while the word EMMP stands for molecular mechanics potential energy in a vacuum. The molecular mechanics force field parameters can be used to determine EMMP using the formula

$$EMMP = EB + ENB \quad (3)$$

whereas ENB stands for nonbonded interactions like electrostatic (EETS) and van der Waals (EVDW) interactions, and EB represents bonded interactions, angle dihedrals, and other variables. Therefore, Eq. (3) can be written as

$$EMMP = EB + (EETS + EVDW) \quad (4)$$

Gsolv can be determined using an implicit solvent model from Eqs. (2a) and (2b). The contribution of electrostatic or polar solvation energy (GP) and nonelectrostatic or non-

polar solvation energy (GNP) to the solvation free energy can therefore be used to express this word. The aforementioned terms are computed by the g_mmpbsa script and the APBS program. Snapshots of the last 10 ns of an MD trajectory were taken in order to complete the aforementioned calculation. The g_mmpbsa program used the extracted snapshots, the tpr, and the index file as input to calculate the binding energy.

## 3.9. Antiviral assay

In this study, I investigated the clinically isolated SFTSV strain KADGH/2013/Korea. This was cultured in Vero E6 cells and has the GenBank accession number KU507553. Real-time RT-PCR was used to calculate the viral following a ten-fold dilution. The Health and Environment Research Institute of Gwangju City's biosafety level-3 laboratory served as the site for all infection studies. The Korean Cell Line Bank (KCLB no. 21587) provided the African green monkey kidney Vero E6 cell line. The Dulbecco's modified Eagle's medium (DMEM, Gibco, Thermo Fisher Scientific, United States) with 10% fetal bovine serum (FBS, Gibco) at 37°C in a humid environment with 5% CO2 was used to preserve cell line.

- **Drugs**

5720 - (2-(10-oxo-10,11-dihydrodibenzo[b,f]thiepin-2-yl )propanoic acid), 75825451- (N-[cis-3-(2-amino-6-oxo-1,6-dihydropyrimidin-4-yl)cyclobutyl]-3-(2methoxyphenyl)-1H-pyrazole-5-carboxamide), 53010325- (N-[cis-3-(2-amino-6-oxo-1,6-dihydropyrimidin-4-yl)cyclobutyl]-5-oxo-1-phenyl-2,5-dihydro-1H-pyrazole-3-carboxamide)

21976453 – (2-amino-7-(tetrahydro-3-furanylcarbonyl)-5,6,7,8-tetrahydropyrido[3,4-d]pyrimidin-4(3H)-one) were purchased from ChemBridge corporation (USA). Favipiravir (T-705) was purchased from Toyama Chemical Co., Ltd. (Japan). 0.22 μM MF-Millipore membrane filter was used to filter the drug solutions and kept at −80°C until further use.

- **Antiviral activity**

Vero E6 cells were used to perform plaque assay. The 12-well culture plates were used. Cells of density $2.5 \times 10^5$ cells/well was injected inside plates for 24 hours in order to investigate the antiviral potency of compounds. Phosphate-buffered saline (PBS) in its sterile form was then used for cell cleaning. $5 \times 10^5$ viral RNA copies/100 plaque forming units (PFUs) of SFTSV were injected to each well. Incubation was done for 1 hour. After the virus was eliminated, cells were 3 times cleaned with PBS. The antiviral compounds then administered to the cells for 48 hours at their maximum plasma concentrations ($C_{max}$) in DMEM mixed with 10% FBS.

- **Plaque Assay**

Vero E6 cells were used to perform plaque assay. The 12-well culture plates were used. Cells of density $2.5 \times 10^5$ cells/well was injected inside plates for 24 hours in order to investigate the antiviral potency of compounds. Then PBS washing was done and exposed for 1 hour to SFTSV at a concentration of 50–100 PFUs per well. The virus was eliminated, and PBS was used three times. The antiviral agents were then administered to the cells in DMEM containing 5% FBS and 1% methylcellulose at 2-fold serial

dilutions of the $C_{max}$ doses. After 10 days of incubation, the growth medium fixation was done by using 1 mL of an (1:1) acetone: methanol solution. Each well received a drop of 1% crystal violet solution and keeping for staining around 20–30 minutes.

- **Data Analysis**

GraphPad Prism 8.0.1 (GraphPad software, San Diego, CA, United States) was used to calculate the $EC_{50}$ of all molecule.

# IV. RESULTS

## 4.1. Diagnosis of SFTSV in clinical samples

A total of 129 whole blood samples were collected from hospitalized patients with suspected SFTS between 2015 and June 2022. These patients experienced clinical manifestations of SFTS. Among 129 SFTS patients, 3 (2.3%) had eschar and 25 (19.4%) deaths were reported. Most number of suspected cases were identified in the Jeolla province (64 of 129 cases), followed by Gyeonggi province (33 of 129), Gyongsang province (25 of 129), Gangwon province (4 of 129), and Chungcheong province (3 of 129). Geographical locations of the sample collection site are mentioned in **Figure 3**. The seasonal distribution of SFTS cases was identified which showed that the month of Summer and Autumn are the most prevalent season for SFTS infection (**Figure 4**).

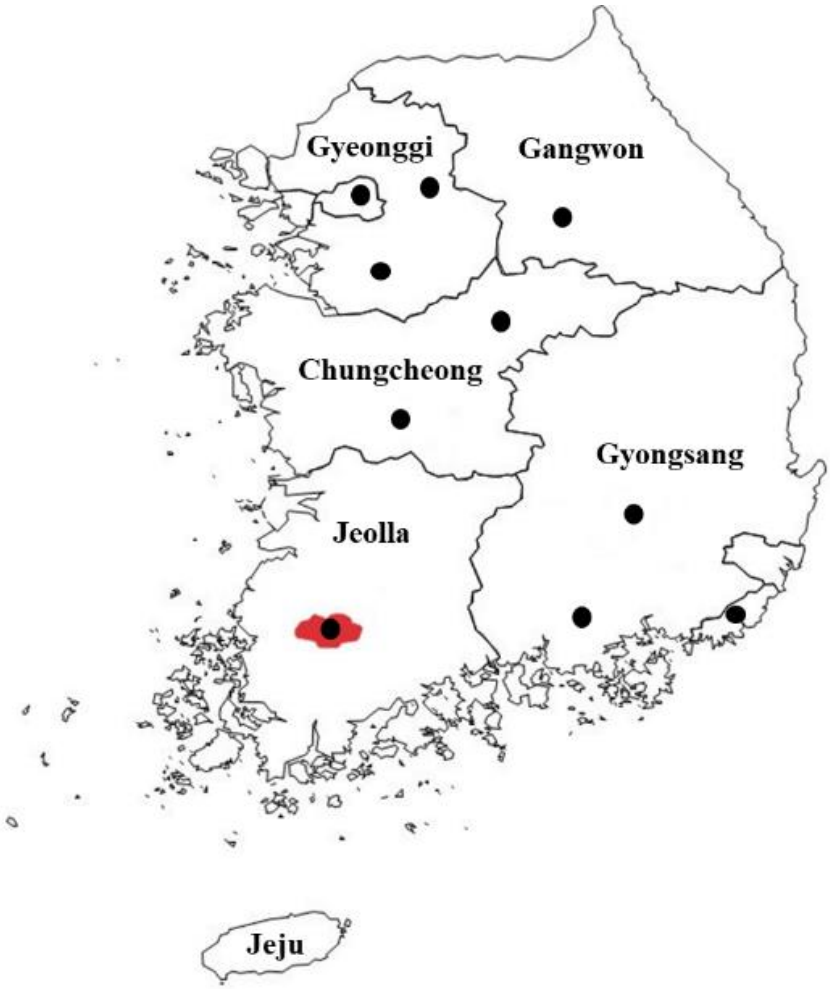


**Figure 3. Geographical location of sample collection sites.** Circle (●) indicates the sample collection sites in each province. Area mark in red indicates the maximum number of samples collected.

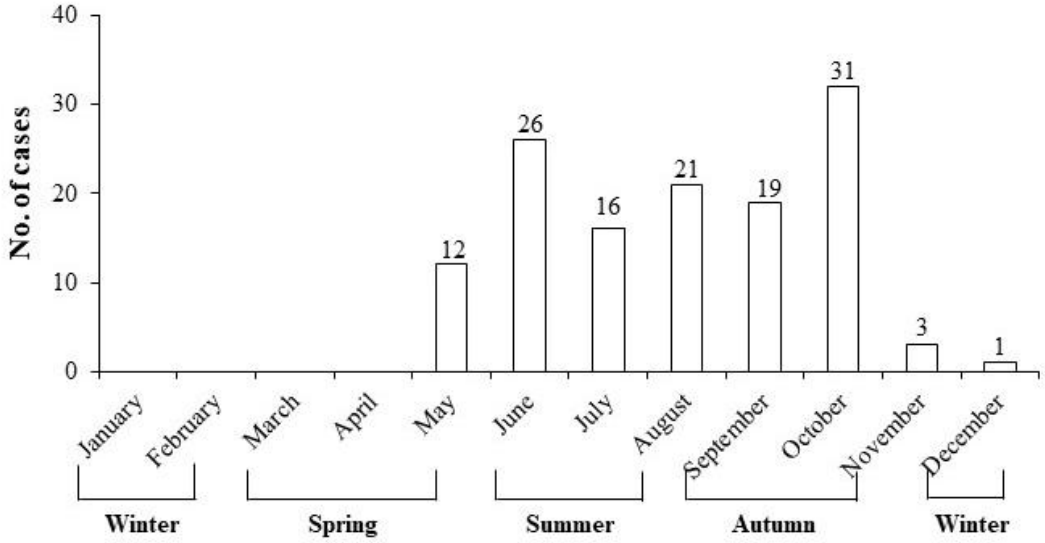


**Figure 4. Seasonal distribution of severe fever with thrombocytopenia syndrome cases identified in our study, 2015-2022**

Overall, specimens from 129 patients were positive for SFTSV by RT-PCR with a case fatality rate of 19.4% (25/129) (**Figure 5**). Patient age ranged between 25 to 92 years, with an average age of 69.4, and majority of the cases were patients aged ≥70 years (**Figure 5A**). Moreover, patients aged ≥70 years showed the highest mortality rate of 29.7% (22 of 74). Patients aged 60-69 years showed fatality rate of 6.5% (2 of 31), and patients aged 50-59 years showed 14.3% (1 of 7) mortality rate (**Figure 5B**). Though I observed no statistically significant age and sex difference in infection or mortality rates due to uneven distribution and smaller number of samples (**Figure 5B and 5C**).

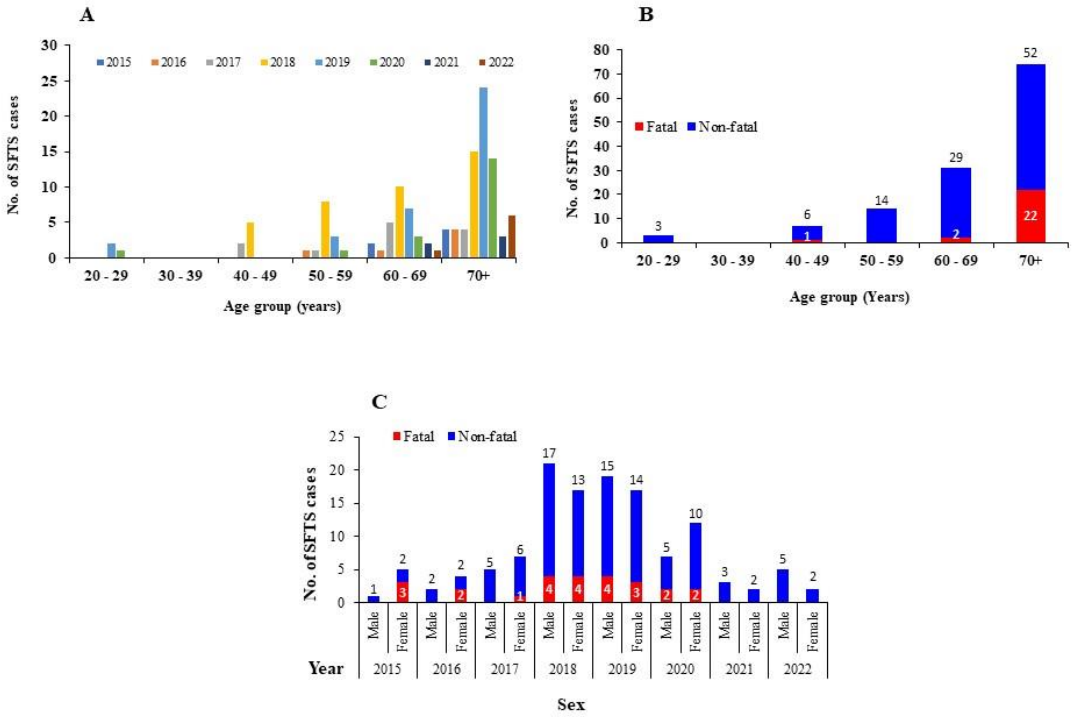


**Figure 5. Distribution of SFTS cases between 2015 to 2022.** A) Age distribution pattern of positive SFTS cases. B) Number of SFTS fatalities in different age group. C) Ratio of non-fatal to fatal cases by sex and year

### 4.1.1 Genetic and phylogenetic analysis

All 129 positive SFTSV sequences were used for analysis. 122 (94.2%) were positive for the partial M segment of the SFTSV RNA genome. 114 (88.4%) were positive for the partial S segment of the SFTSV RNA genome. Phylogenetic analysis was performed using these sequences as well as reference sequences available in GenBank (**Figure 6 and Figure 7**).

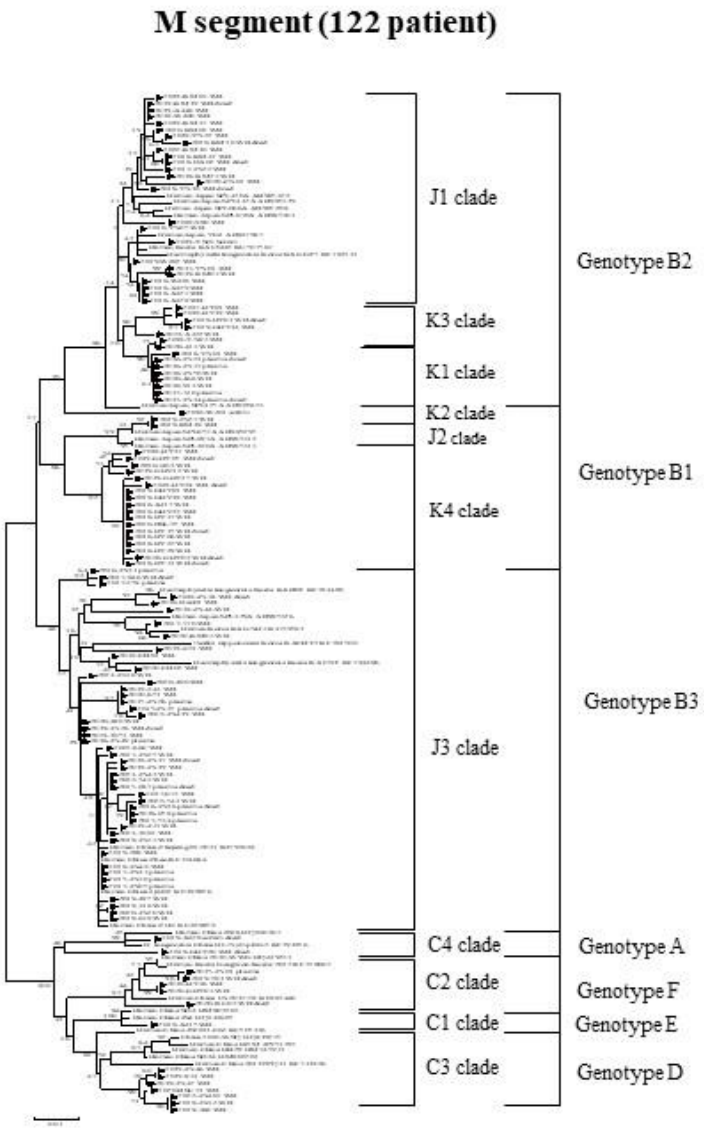


**Figure 6. Phylogenetic tree constructed on the basis of SFTS virus M segment (477 bp) gene sequences for SFTS patients in Korea (►) and GenBank reference sequences**

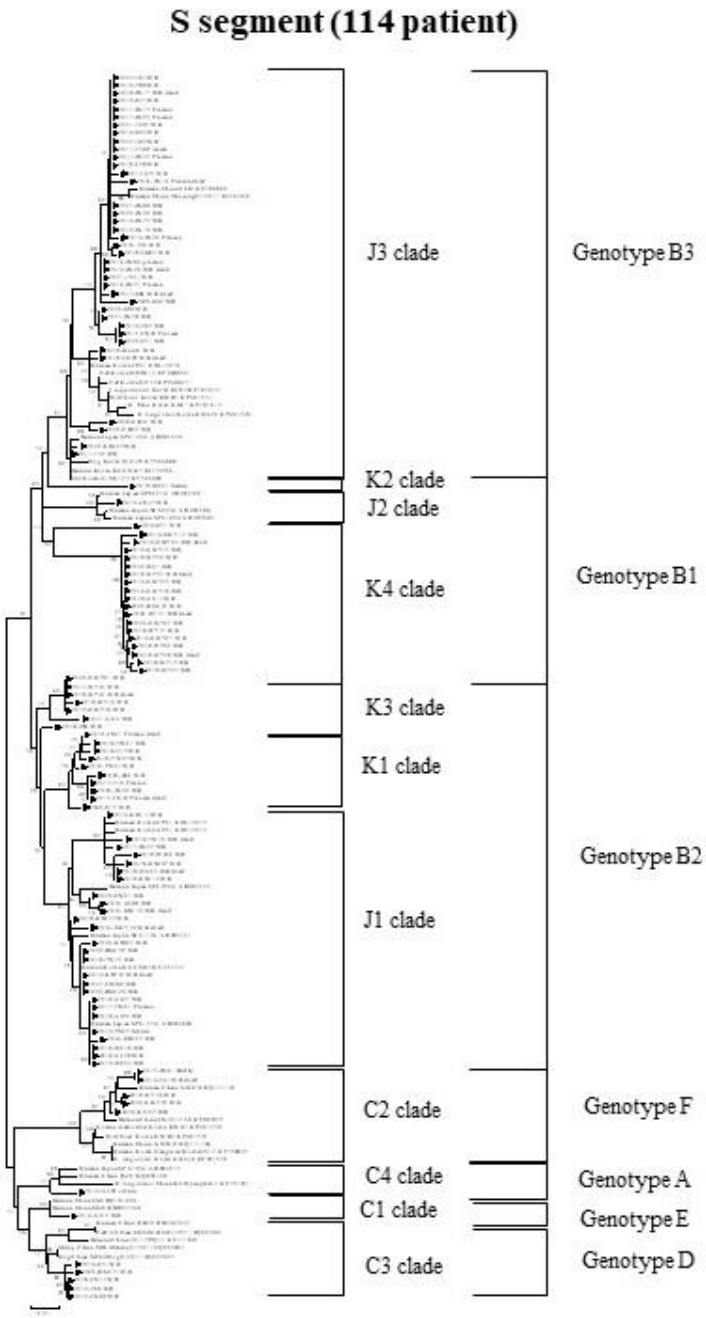


**Figure 7. Phylogenetic tree constructed on the basis of SFTS virus S segment (321 bp) gene sequences for SFTS patients in Korea (►) and GenBank reference sequences**

Results from the phylogenetic analysis revealed that Korean SFTS virus distinguished into genotypes A-F which is similar to Korea and China [5,69]. Among these, B-3 (n = 46, 35.7%) was the most prevalent genotype, then B2 (n = 45, 34.9%), and B-1 (n = 21, 16.3%). Among B-2 genotype, clade J1 (Japan clade 1) was more prevalent (n = 28, 21.7%) than Korea clade K1 (n = 11, 8.5%), and K3 (n = 6, 4.7%). Among B-1 genotype, Korea clade K4 (n = 18, 13.9%) was more prevalent than K2 (n = 1, 0.8%), and J2 (n = 2, 1.6%). The clade-based SFTSV geographical distribution map revealed that, genotype B-2 SFTSV strain was more prevalent in Gangwon province endemic area. B-1 and B-2 genotype were associated with high mortality rate in Gyeonggi province. Further, genotype B-3 was more prevalent in Jeolla province which presented high risk factor in this endemic area with high mortality rate (**Figure 8**).

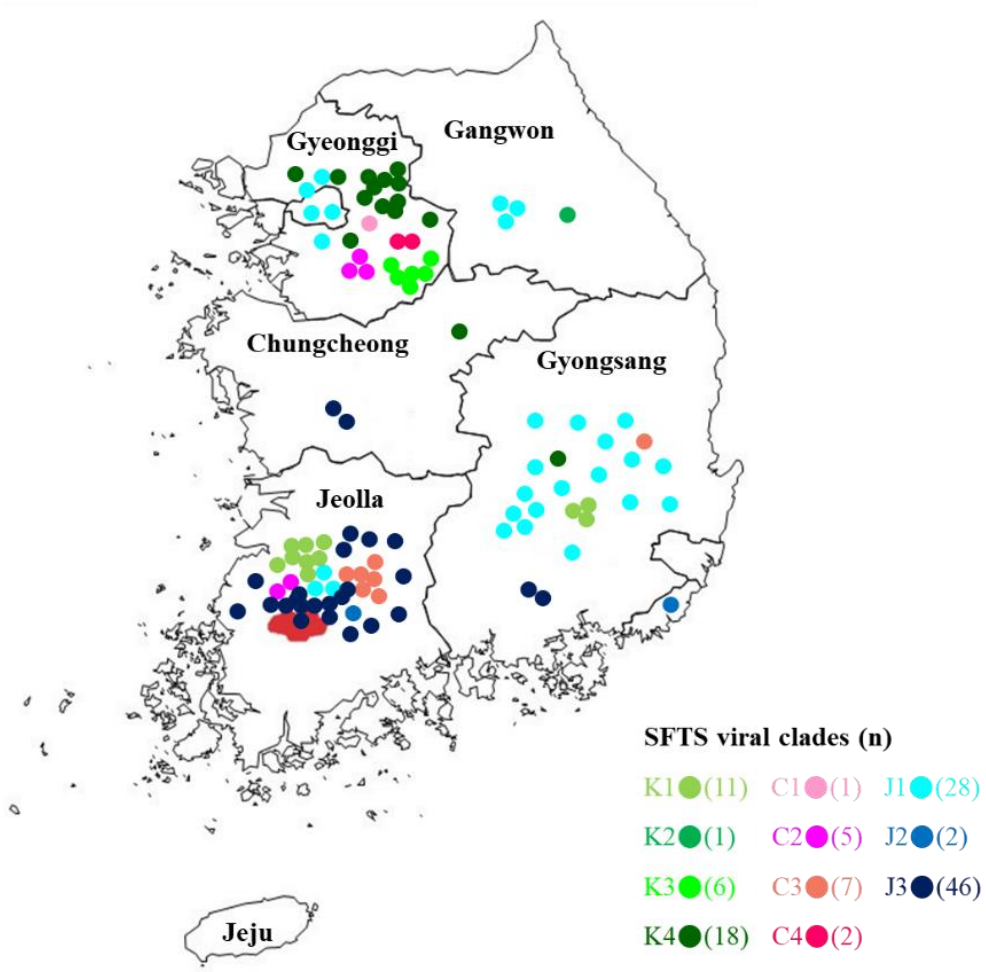


**Figure 8. The clade-wise distribution characteristics of SFTSV**

The circles showed the distribution of each SFTSV clades in the five provinces of South Korea. Each color indicated the related SFTSV clade according to the graphic symbol

Moreover, genotype F (n = 5, 3.9%) which was first identified in 2012 was also detected in this study but in low prevalence than B-1, B-2, B-3, and D genotype. Additionally, genotype D which was prevalent in 2013 and 2014, in recent years, only few cases have been detected (n = 7, 5.4%). Moreover, only 2 cases of genotype A (1.6%) and 1 cases of genotype E (0.8%) were identified in this study. In contrast, genotype C was not identified in this study. In Japan, B-2 genotype was most prevalent which is different than our study. Also, genotype F was the most prevalent in China among 14 reported SFTSV strains which was low in prevalence in our study.

Further detailed investigation revealed the presence of 4 reassortant group genotypes of SFTSV (**Figure 9**).

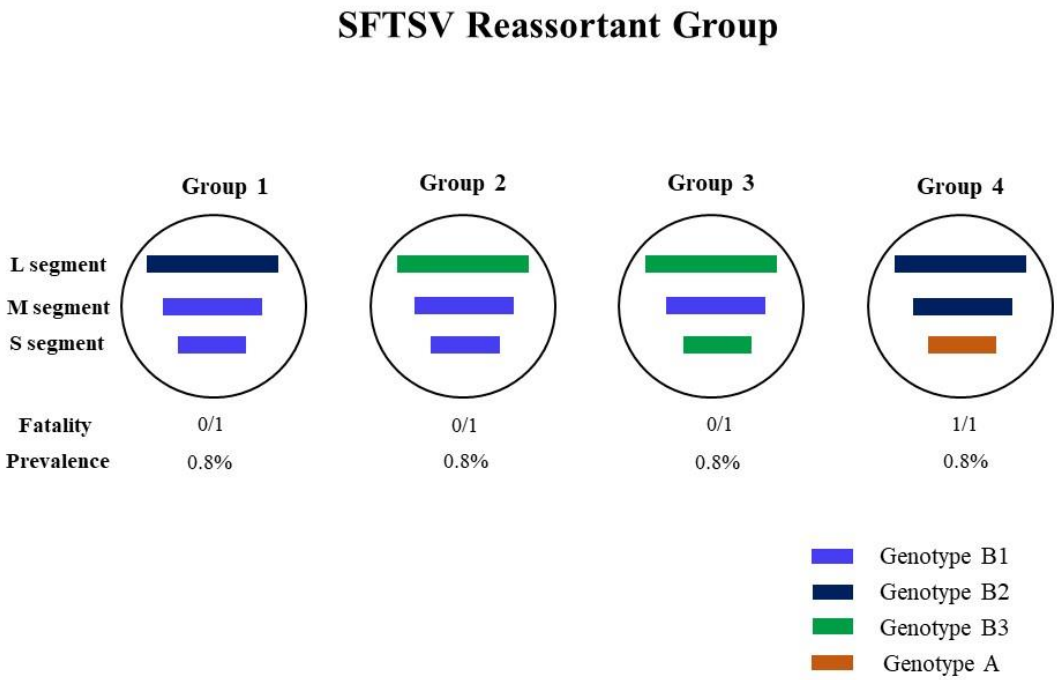


**Figure 9. Genotype reassortant of SFTSV strains.**

The SFTSVs were categorized into different genotypes based the phylogenetic analysis. 4 genetic reassortant viruses were identified in this study: reassortant group 1, group 2, group 3, and group 4. Gene segments from top to bottom are L, M, and S. The bars indicate reassortant groups of genotypes. The case fatality rate and SFTS prevalence were mentioned with each reassortant genotypes of SFTSV.

In this study, I observed the presence of various reassortants in a single strain. Among 4 reassortant groups, group 1 consists of B-2 and B-1 genotypes, group 2 and group 3 contained genotype B-3 and B-1, and group 4 has genotype B-2 and genotype A. These findings imply that the Korean SFTSV strains were dynamically evolving through active reassortments that yielded a variety of new genotypes.

### 4.1.2. SFTSV genotypes and mortality

To analyze the different SFTSV genotypes induced mortality rate, I investigated the human case fatality rate across genotypes identified in our study (**Figure 10**). Most genotypes were identified annually (2015-2022), but genotype A and E were only detected in 2019 with low incidence (**Figure 10A**). Even though I observed that the most genotypes were related with mortality rate, genotype B-1 showed highest mortality rate of 23.8% (5 of 21), followed by B-2 of 17.8% (8 of 37), and B-3 with 17.4% (8 of 38) (**Figure 10D**). Genotype A and F also showed higher mortality rate of 100% and 40% respectively but the prevalence rate was only 1.6% (2 of 129) for genotype A and 3.9% (5 of 129) for genotype F. In our study, no mortality associated with genotype D and E was observed. Among reassortant groups, only group 4 was associated with mortality (1 of 1 case, 100%). Although only single cases of each of the reassortant genotype was detected in this study. Moreover, I identified a significant difference in the fatality rate between different age group of infected patients (**Figure 10B**). Patients aged >70 years (22 of 74, 29.7%) showed the higher fatality rate than the patients aged

below 70 years (3 of 55, 5.5%) (*P<0.05*). No significant sex and genotype differences in the SFTS infection or mortality rates were observed (**Figure 10C and Figure 10D**).

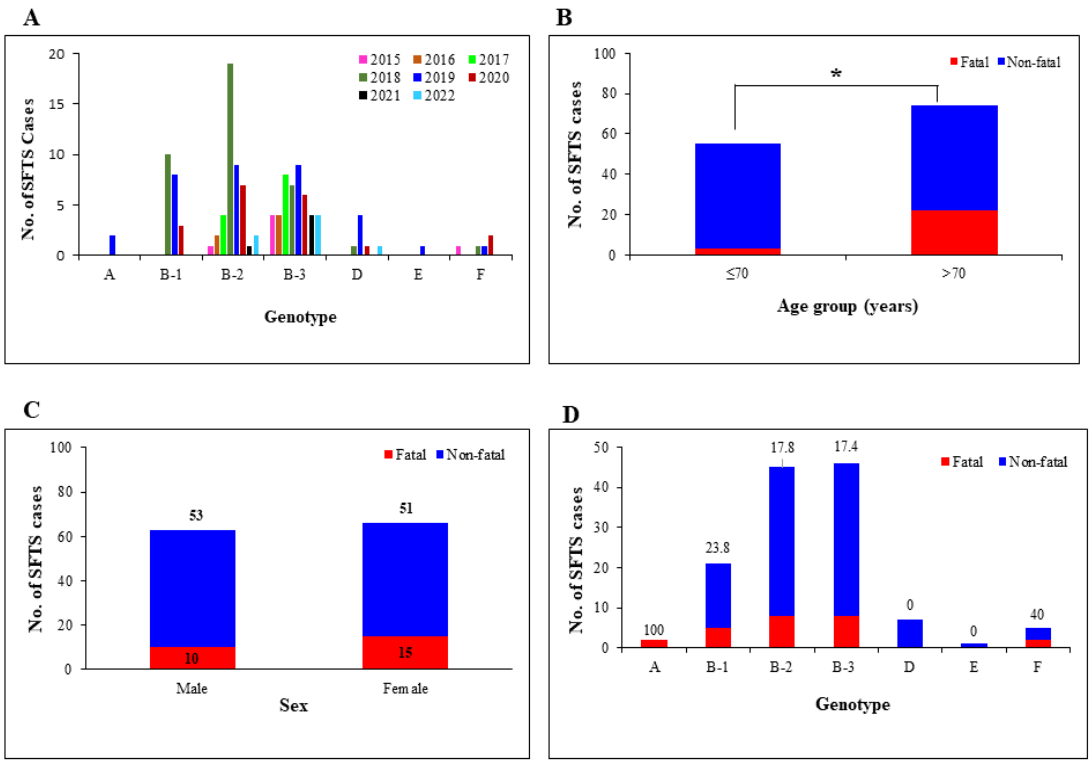


**Figure 10. Year-wise SFTS prevalence and fatality rate of each SFTSV genotypes**

(A) Number of each genotype of SFTSV from 2015 to 2022. (B) Case fatality ratio by each age group. (C) Case fatality ratio by each sex. (D) Case fatality ratio for each SFTSV genotype. The fatality rates (%) is mentioned at the top of each bar. Asterisk indicate statistically significant differences in mortality rates between each aged group (C) determined by Fisher's exact test (*$P < 0.05$).

## 4.2. Assessment of coinfection of SFTS with scrub typhus

To investigate the frequency of coinfection in suspected SFTS patients infected with tick-borne diseases, I performed RT-PCR to analyze the possible coinfection associated with it.

### 4.2.1. Characteristic of scrub typhus patients

Among the 2 coinfected patients, 1 patient was female (patient 1) aged 79 and another was male (patient 2) aged 64. Detailed clinical characteristics and outcomes of these 2 patients with coinfection are shown in **Table 3**. Patient 1 was diagnosed with SFTS in November 2019 with a presentation of skin rash and eschar. Patients' IgM antibody titer for *O. tsutsugamushi* was observed to be 1:64 and showed positive results for both the PCR targeting 56-kDa antigen gene as well as *tchA* Q-PCR. Patient 2 was diagnosed with SFTS in June 2022 whose whole blood sample showed positive result for scrub typhus nested PCR as well as Q-PCR but the subsequent sample IFA showed negative outcome. Both the coinfected patients presented with fever but only one of them had eschar and skin rash which makes the clinical differentiation of coinfection or single infection more difficult.

**Table 3. Clinical characteristics and outcomes of two coinfected patients**

| Variables | Patient 1 | Patient 2 |
|---|---|---|
| Age, year | 82 | 64 |
| Gender | Female | Male |
| **Comorbidities** | DM<br>CVA | Chronic liver disease |
| **Geographical location in Korea** | Jeolla province | Jeolla province |
| **Onset of illness to admission, day** | 8 | 0 |
| **APACHE II score** | 7 | NA |
| **Symptoms and signs** | | |
| Fever | Yes | Yes |
| Headache | None | None |
| Myalgia | None | None |
| Nausea/vomiting | None | None |
| Arthralgia | None | None |
| Regional lymphadenopathy | None | None |
| Abdominal pain | None | None |
| Altered mentality | None | yes |
| **Skin presentation** | | |
| Eschar | Yes | None |
| Skin rash | Yes | None |
| **Laboratory findings** | | |
| White blood cell, /mm³ | 7200 | 3700 |
| Leukopenia (< 4,000/mm³) | None | Yes |
| Hemoglobin, g/dL | 11.4 | 14 |
| Anemia (< 11 g/dL) | None | None |
| Platelet, ×1000 /mm³ | 55 | 162 |
| Thrombocytopenia (< 150,000/mm³) | Yes | None |
| Severe thrombocytopenia (< 50,000/ mm³) | None | None |
| C-reactive protein, mg/dL | 10.72 | 0.94 |
| AST, IU/L | 72 | 50 |
| ALT, IU/L | 34 | 47 |
| Total bilirubin, mg/dL | 0.55 | 0.46 |
| LDH, IU/L | 710 | 887 |

| Clinical course | | |
|---|---|---|
| Intensive care unit admission | None | None |
| Mechanical ventilation | None | None |
| Hospital stays (days) | 13 | 11 |
| Death (%) | None | None |
| ***O. tsutsugamushi* IFA titer** | 1:64 | Negative |
| PCR for *O. tsutsugamushi* | Positive | Positive |
| PCR for SFTSV | Positive | Positive |

DM: Diabetes Mellitus; CVA: cerebrovascular accident; APACHE II: Acute Physiology and Chronic Health Evaluation; AST: aspartate aminotransferase; ALT: alanine transaminase; LDH: Lactate Dehydrogenase

### 4.2.2. Prevalence of coinfection of SFTS with scrub typhus

From the 129 samples, 2 patients with confirmed SFTS showed positive nested PCR results for *O. tsutsugamushi* which was further investigated by sequencing analysis. The BLAST results showed 100% identity for *O. tsutsugamushi* sequences. The geographical location of the suspected regions of coinfection was mentioned in **Figure 11**. The prevalence of coinfection was observed to be 1.6% (2/129) (95% CI, 0.001–0.06). Both the cases of coinfection were observed in southern area of Jeolla province. Coinfection with anaplasmosis and leptospirosis were not observed in any patient. I compared results of phylogenetic analysis of both the 56-kDa gene sequences with 28 reference sequences. Phylogenetic tree revealed that two strains identified in this study were clustered with strain Boryong isolated in Seoul city, Korea (**Figure 12**).


**Figure 11. Geographical location of the observed SFTS and scrub typhus coinfection (area in red)**

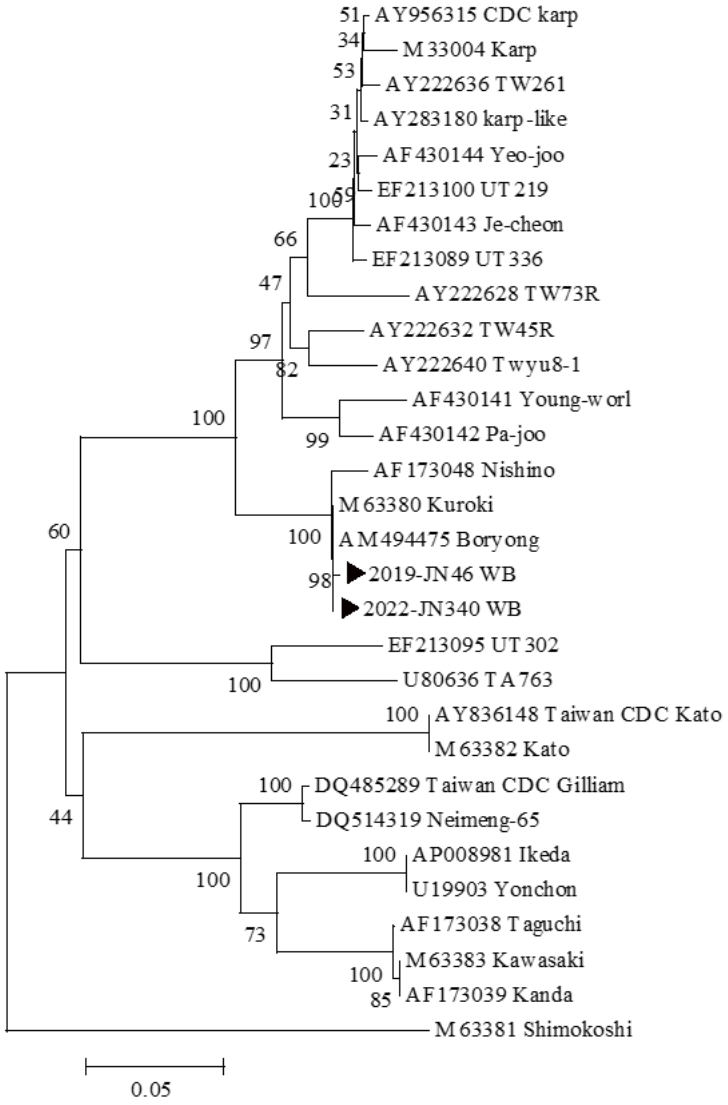


**Figure 12. Phylogenetic tree constructed on the basis of *Orientia tsutsugamushi* 56-kDa gene sequences (439bp) for scrub typhus patients in Korea (►) and GenBank reference sequences**

## 4.3. Assessment of coinfection of SFTS with spotted fever group rickettsia infection

### 4.3.1. Characteristic of rickettsiosis patients

Among the 8 coinfected patients, 3 patients were men, 5 patients were female, and average age was 73 (range, 49-92). Detailed clinical characteristics and outcomes of these 2 patients with coinfection are shown in **Table 4**. The co-infected patients showed similar clinical signs compared to SFTS only patients. The longest period from the beginning of the first fever to the serum collection was 5 days. Among all the coinfected patients, only one had skin rash but no sign of eschar which makes the clinical differentiation of coinfection or single infection more difficult. Most cases were observed in July (4 of 8, 50%), followed by June (3 of 8, 37.5%), and October (1 of 8, 12.5%).

**Table 4. Clinical characteristics and outcomes of the eight coinfected patients**

| Variables | Patient 1 | Patient 2 | Patient 3 | Patient 4 | Patient 5 | Patient 6 | Patient 7 | Patient 8 |
|---|---|---|---|---|---|---|---|---|
| Age, year | 49 | 72 | 82 | 70 | 78 | 80 | 92 | 61 |
| Gender | Female | Male | Female | Female | Female | Male | Female | Male |
| Comorbidities | None | None | None | None | None | None | None | None |
| Geographical location in Korea | Gyeonggi province | Gyongsang province | Jeolla province | Jeolla province | Jeolla province | Gyeonggi province | Gyeonggi province | Gyeonggi province |
| Onset of illness to admission, day | 3 | NA | 2 | 1 | 3 | NA | NA | NA |
| Symptoms and signs | | | | | | | | |
| Fever | Yes | NA | Yes | None | None | NA | NA | NA |
| Headache | None | NA | None | None | Yes | NA | NA | NA |
| Myalgia | Yes | NA | None | None | Yes | NA | NA | NA |
| Nausea/vomiting | None | NA | None | None | None | NA | NA | NA |
| Arthralgia | Yes | NA | None | None | Yes | NA | NA | NA |
| Regional lymphadenopathy | None | NA | None | None | Yes | NA | NA | NA |
| Abdominal pain | None | NA | None | None | Yes | NA | NA | NA |
| Altered mentality | None | NA | None | None | None | NA | NA | NA |
| Skin presentation | | | | | | | | |
| Eschar | None | None | None | None | None | None | None | None |
| Skin rash | Yes | None | None | None | None | None | None | None |
| Laboratory findings | | | | | | | | |
| White blood cell, /mm³ | 2700 | NA | 2860 | 1420 | 5130 | NA | NA | NA |
| Leukopenia (< 4,000/mm³) | Yes | NA | Yes | Yes | 0 | NA | NA | NA |

| | | | | | | | | |
|---|---|---|---|---|---|---|---|---|
| Hemoglobin, g/dL | 14.5 | NA | 12.3 | 11.4 | 14.1 | NA | NA | NA |
| Anemia (< 11 g/dL) | No | NA | None | None | None | NA | NA | NA |
| Platelet, ×1000 /mm³ | 111 | NA | 102 | 102 | 52 | NA | NA | NA |
| Thrombocytopenia (< 150,000/mm³) | None | NA | None | None | Yes | NA | NA | NA |
| Severe thrombocytopenia (< 50,000/ mm³) | None | NA | None | None | None | NA | NA | NA |
| C-reactive protein, mg/dL | 0.11 | NA | 1.57 | NA | 0.020 | NA | NA | NA |
| AST, IU/L | 70 | NA | 117.6 | 144.7 | 284 | NA | NA | NA |
| ALT, IU/L | 37 | 68.2 | 27.3 | 74.2 | 107 | NA | NA | NA |
| Total bilirubin, mg/dL | 0.2 | NA | 0.15 | 0.16 | 0.240 | NA | NA | NA |
| LDH, IU/L | 0 | NA | NA | 718 | 2605 | NA | NA | NA |
| Clinical course | | | | | | | | |
| Intensive care unit admission | None | None | None | None | None | Yes | None | None |
| Mechanical ventilation | None | None | None | None | None | Yes | None | None |
| Hospital stays (days) | 4 | NA | 22 | 12 | 10 | NA | NA | NA |
| Death (%) | None | NA | None | None | None | Yes | Yes | None |
| PCR for *Rickettsia spp.* | Positive | Positive | Positive | Positive | Positive | Positive | Positive | Positive |
| PCR for SFTSV | Positive | Positive | Positive | Positive | Positive | Positive | Positive | Positive |

NA: Not available

### 4.3.2. Prevalence of coinfection of SFTS with rickettsiosis

From the 129 samples, 8 patients with confirmed SFTS showed positive nested PCR results for *rickettsia* spp. which was further investigated by sequencing analysis. The BLAST results showed 100% identity for *rickettsia* sequences. The frequency of coinfection was in order of Gyeonggi province (4 of 33, 12.1%), Jeolla south province (3 of 64, 4.7%), and Gyongsang province (1 of 25, 4%) (**Figure 13 and Table 4**). Farm fields dominated most of these areas. The variability in sample sizes in each region, however, prohibited direct statistical comparison. Anaplasmosis and leptospirosis co-infection tests for every patient in this investigation came out negative. I compared results of phylogenetic analysis of both the *ompA* gene sequences with other reference GenBank sequences. Phylogenetic tree analysis showed that among 8 identified sequences, 7 sequences found in our study were closely clustered with *Rickettsia monacensis* and 1 sequence formed cluster with *Rickettsia tamurae* strain (**Figure 14**). The prevalence of coinfection of SFTS with SFG was estimated to be 6.2% (95% CI, 0.03–0.13).


**Figure 13. Geographical location of observed SFTS-rickettsiosis coinfection (area in red)**

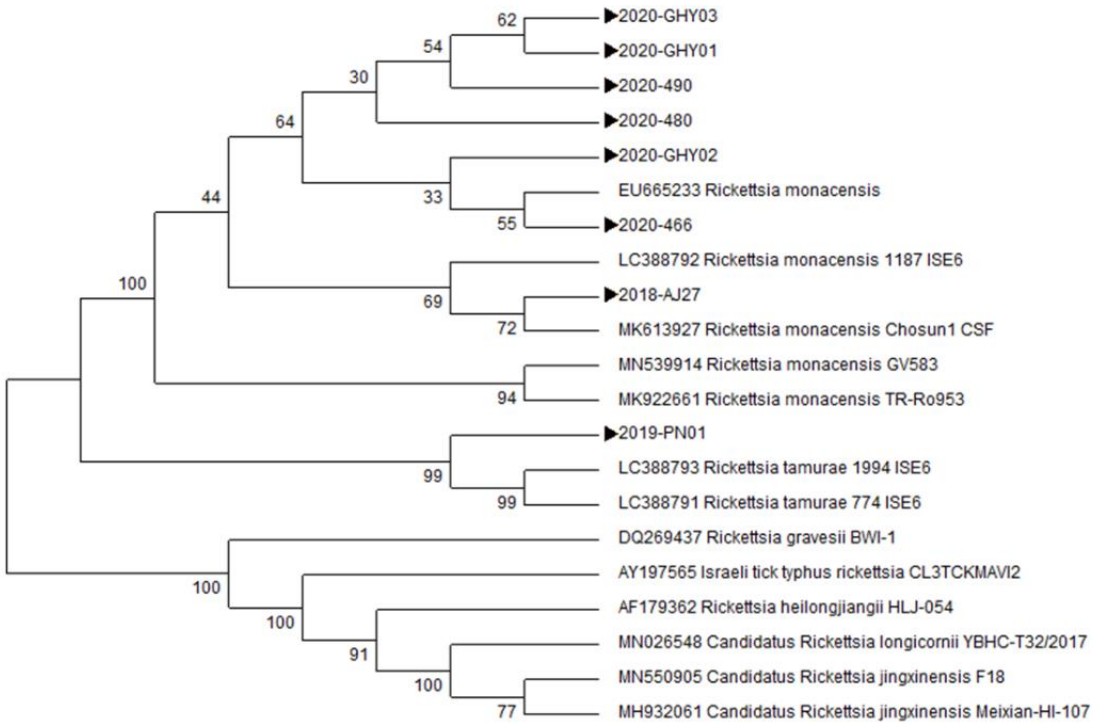


**Figure 14. Phylogenetic tree constructed on the basis of *rickettsia* spp. outer membrane protein A (ompA - 380bp) gene sequences for rickettsiosis patients in Korea (►) and GenBank reference sequences**

## 4.4. In-silico analysis

### 4.4.1. Docking validation and virtual screening

The SFTS L protein was docked with a variety of co-crystalline ligands in the current study. Ten conformations or docking postures were produced by the docking algorithm. Each docking pose was overlaid over MGP (co-crystalline orientation). The docking value came out as − 6.8 kcal/mol, and the associated RMSD was found to be ~ 1.8 Å (**Figure 15**). The MGP and co-crystalline ligand interaction revealed H-bonding and hydrophobic contacts with the amino acids Glycine1707, Aspartic acid1771, and Leucine1772. Further, π–π-stacking with Pro1ine706, Isoleucine1738, and Isoleucine1774 (**Figure 15**). The docking protocol's validity was significantly backed up by the RMSD and interaction analyses [70]. Any small-molecule medication that shown interactions with those above-mentioned amino acids and a Vina docking value ≥7-.0 kcal/mol was rank-wise nominated. π–π-type bonding was the crucial one. In order to create a condensed list of small compounds from both databases, the aforementioned hypothesis was tested.

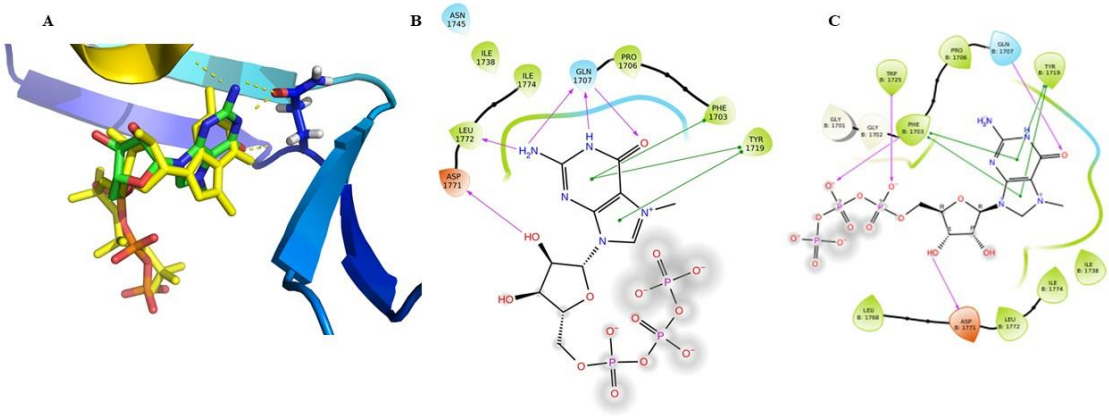


**Figure 15. Docking validation between SFTSV L protein and co-crystalline ligand MGP**

15A) Orientation of co-crystalline ligand where green color ligand= native pose, yellow color ligand=docking conformation. RMSD=1.8Å, 15B) hydrogen bond interaction between protein ligand system, and 15C) hydrophobic bond interaction between protein ligand system

Docking program Autodock Vina was used. The docking procedure was run by a custom bash script to screen out a large number of molecules. The best four ligands showed value of -8.7, -8.5, -8.2, and -8.0 kcal/mol. These were compound A (ID-5720), compound B (ID-75825451), compound C (ID-53010325), and compound D (ID-21976453). The majority of ligands displayed hydrophobic and hydrogen bond contacts with those amino acids. The different characteristics of all potential receptor-ligand combination were also explored using a 100 ns MD simulation.

### 4.4.2. Molecular dynamics (MD) simulation and identification of potential hit against SFTSV

The scientific community generally accepts MD simulation as a method of evaluating the permanent binding of a protein-ligand interaction. From the whole 100 ns MD trajectory, each frame's RMSD values were determined and plotted versus time (Figure 16). The RMSD parameter, which is computed from the MD analysis, indicates the changes that take place in a protein structure's geometric orientation. A globular protein has improved stability when its RMSD is smaller than 3 Å [63,71].

It is clear from the average RMSDs that each hit oscillates at a RMSD lower than Apo protein (RMSD ~ 1.63 Å). A thorough examination of **Figure 16** reveals that none of the indicated candidate systems experience rapid RMSD profile shifts. The RMSF characteristics were then determined in order to comprehend the nature of specific residues throughout the MD simulation. The average RMSF of each system is less than that of the apo protein.

The radius of gyration (Rg) explains the compactness of a protein system [65]. It's possible that the protein system is robust and doesn't undergo any substantial structural aberrations or changes throughout the simulation, according to a consistent Rg profile. In order to comprehend how Rg varies over time, a plot was created (**Figure 16**).

There haven't been any noticeable changes to the Rg profile. According to the aforementioned findings, it can be concluded that with each of the identified potential ligands, the SFTS L protein forms a stable compound while maintaining its geometric

alignment in each system. The SASA value estimated out from MD curve offers insight into to the activities at the protein-ligand interface. Lower SASA values indicate that the ligand is concealed within the binding domain [66]. In this study, all ligands showed SASA values lower than the only protein system which proved that every ligand lies within the receptor pocket (**Figure 16**). The 100 ns MD trajectory was also used to compute the binding energy such as MMPBSA. A ligand's stable binding to a protein is indicated by highly negative binding energy [54]. Each ligand appears to bind the SFTS L protein with stability. Additional evidence for this claim can be found in data on additional metrics derived from the MD trajectory, such as RMSD, RMSF, Rg, and SASA.

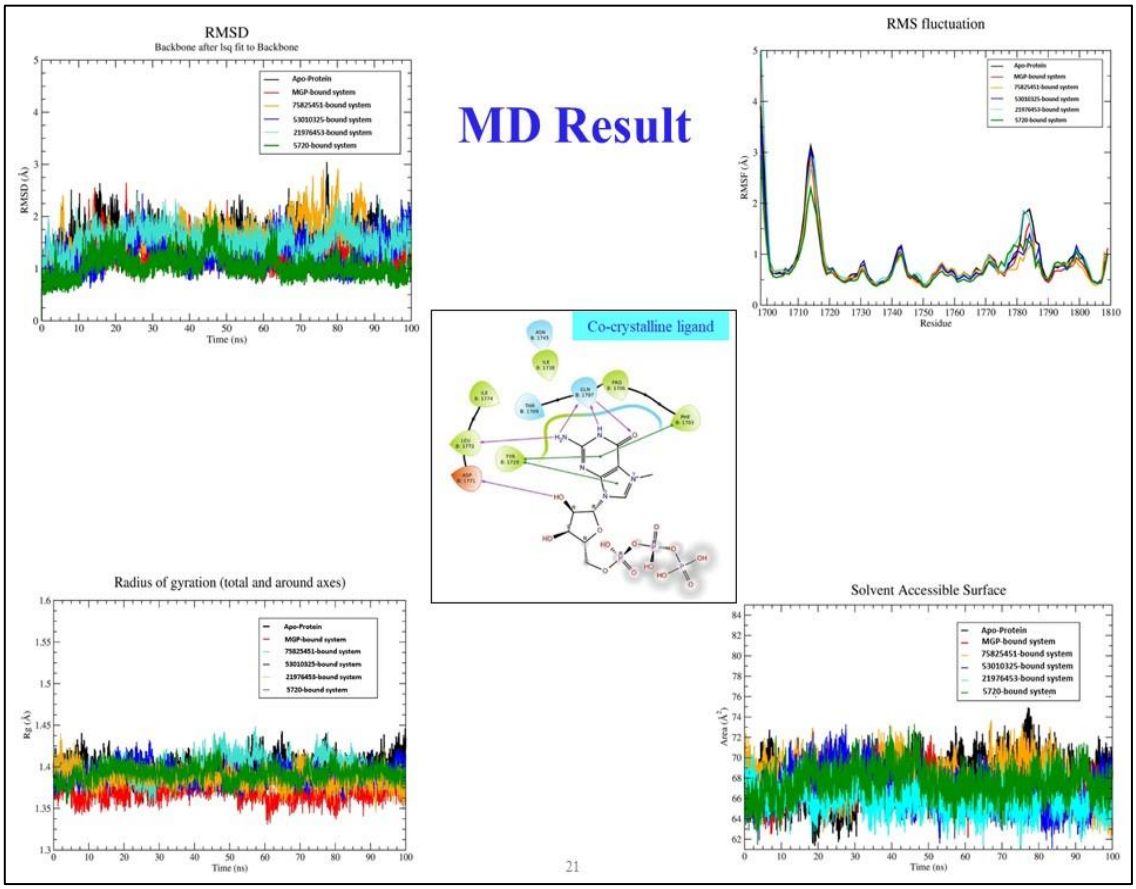


**Figure 16. Graph depicted the molecular dynamic parameters for all identified compounds in this study**

## 4.5. Antiviral assay

The antiviral activity of the four compounds was determined by plaque assay after treating with the compounds at highest concentration of 100μg/mL and 2-fold serial dilution of it. The minimum concentration at which the compound can inhibit 50% of the viral replication was calculated by comparing with the control group (no drug treatment). The concentration of the compounds which inhibited SFTSV by 50% were: Favipiravir, $EC_{50}$ 4.14μg/mL (26.4 μM); ID 5720, $EC_{50}$ 25.58μg/mL (85.7 μM); ID 75825451, $EC_{50}$ 110.5μg/mL (290.5 μM); ID 53010325, $EC_{50}$ 204.3 μg/mL (557.6 μM); ID 21976453, $EC_{50}$ 98.69 μg/mL (373.4 μM). Only Favipiravir which was used as a positive control, showed 50% inhibition at a concentration below $C_{max}$ (**Figure 17**). Other four compounds found to have only 30-40% inhibitory effects on the SFTSV at highest concentrations (**Figure 18**).

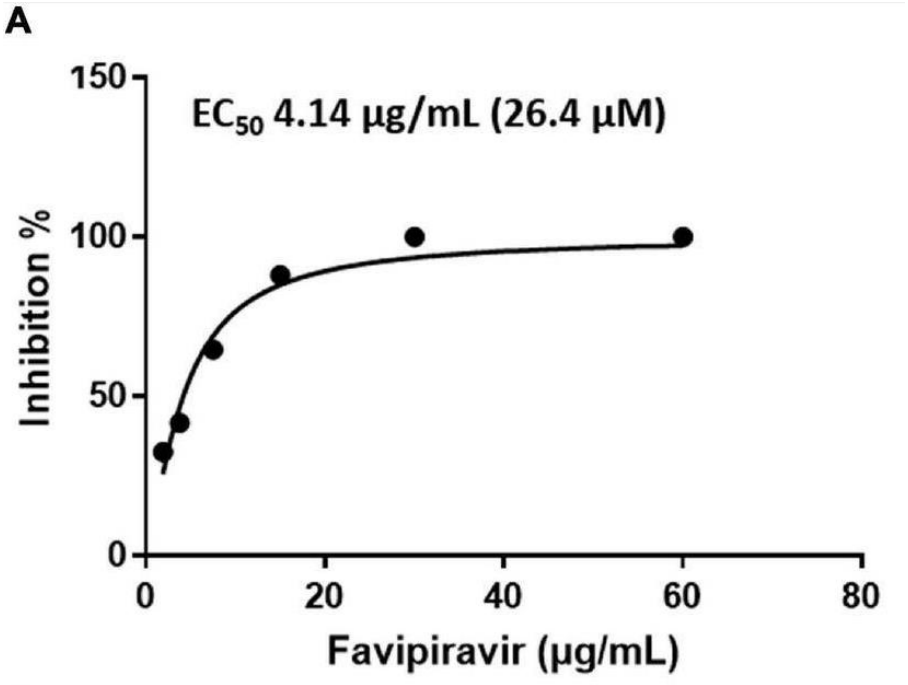


**Figure 17. Efficacy of favipiravir in inhibiting SFTSV replication in Vero E6 cells as determined by plaque assay.**

Graph describe mean inhibition (%) of SFTS viral plaques (left y-axis) in the presence of the antiviral compound favipiravir (positive control). Vero E6 cells were infected with 50–100 PFUs of SFTSV in the presence favipiravir for 10 days.

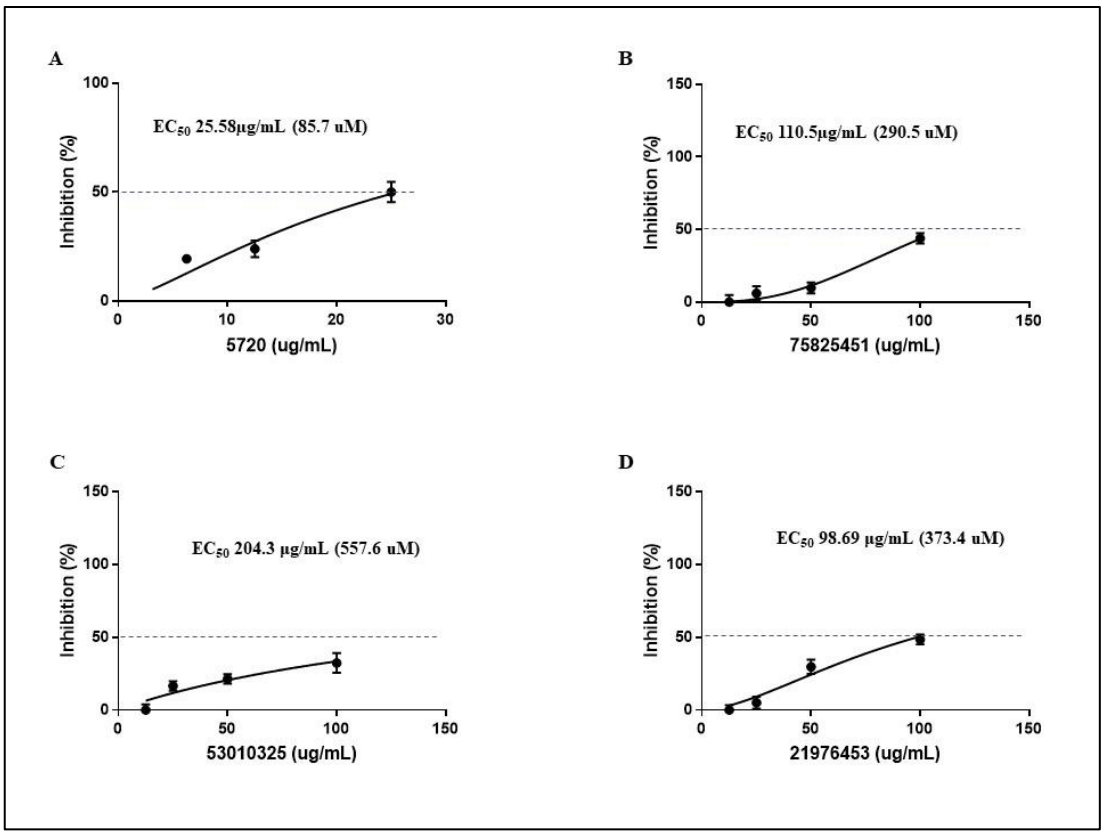


**Figure 18. Efficacy of the molecules in inhibiting SFTSV replication in Vero E6 cells as determined by plaque assay**

Graphs describe mean inhibition (%) of SFTS viral plaques (left y-axis) in the presence of the antiviral compounds (A) 5720, (B) 75825451, (C) 53010325, and (D) 21976453. Vero E6 cells were infected with 50–100 PFUs of SFTSV in the presence of a compound for 10 days

# V. DISCUSSION

Since its discovery, SFTSV has been reported in more than 25 Chinese, Japanese, and South Korean provinces [72, 73], and some new phlebovirus with similar evolutionary relationships to SFTSV have also been recognized in the USA [74], Australia [75], and India [76]. These findings have increased the importance of SFTSV and its significance for global public health issues. The World Health Organization (WHO) classified SFTSV as a virus of highest concern in 2016 and 2017. To learn more about SFTSV epidemiology and genetic traits, it is imperative to expedite the research of molecular evolution analyses for this novel, highly deadly bunyavirus. Therefore, in this study I evaluated the genetic and epidemiological variety of SFTSV strains in South Korea. Further, I investigated the frequency of possible coinfection associated with SFTS and other zoonoses and targeted the SFTSV genome to identify suitable therapeutic target against it.

A total of 382 suspected SFTSV specimens were gathered from 14 hospitals across South Korea during the period of study, and 129 individuals, mostly elderly, had their SFTSV infection verified. According to epidemiological analysis of SFTS cases, 25 (19.4%) cases were fatal, and the majority of the patients in these cases were at least 50 years old. The findings of related studies are consistent with the high frequency and high mortality rate among the elderly revealed here [77]. Further, I performed the phylogenetic analysis of 129 SFTSV positive sequences and reference sequences that showed the genotypic classification of Korean SFTSV. Moreover, B genotype can

further be grouped into B-1, B-2, and B-3 [5, 69]. However, in contrast to previous studies, C genotype was not identified in our study [5, 69]. Data revealed that the B-3 (n = 46, 35.7%) genotype was the most prevalent in South Korea, then B-2 (n = 45, 34.9%) and B-1 (n = 21, 16.3%) (Figure 3A). Incidence of D (n = 7), F (n = 5), A (n = 2), and E (n = 1) genotypes were very less. The greatest number of mortality and occurrence rates were observed in genotype B-1 genotype (23.8%, 5 of 21). Genotype A and F also showed higher mortality rate of 100% and 40% respectively but the prevalence rate was only 1.6% (2 of 129) for genotype A and 3.9% (5 of 129) for genotype F. Moreover, the inconsistency in the phylogenetic clustering revealed that at least 7 genotypes and 4 reassortant group were co-circulating in different endemic areas of South Korea. It is thought that the segmented genomic characteristics of bunyaviruses contributed to the genetic reassortment that resulting in viral evolution [78]. Previously, many studies were performed which showed the evidence of genetic reassortment in SFTSV in China, Japan, and Korea but in this study, I first identified the 4 different types of reassortment group genotypes co-circulating in South Korea [78,79]. This suggests the dynamic evolutionary nature of the SFTSV strains to create novel genotypes which makes the diagnosis more difficult.

In East Asia, the reported average overall mortality rate for SFTSV infections varied substantially, with China reporting a rate of 5.3%-16.2%, Japan reporting a rate of 20%, and South Korea reporting a rate of 23.3% [80-82]. The disparity in reported case death rates may therefore be related to the varied distribution of SFTSV genotypes among

nations, according to a comparison of viral genotype and mortality rates. An interesting genetic study of reported full-length sequences revealed that the most prevalent genotype in Japan was B-2, having a persistent high mortality rate. No cases of Genotype A and F were observed. On the other hand, genotypes F (44.3%) and A (21.5%) in Korea both displayed comparatively low case mortality rates, but the most common genotypes in China [83]. These results suggest that in addition to patient age, the prevalence of different genotypes in each region may also contribute to the different mortality rates between countries. Overall, the epidemiological and genetic investigation on SFTSV increases our knowledge towards the diverse genomic and pathogenic character of SFTSV in South Korea. Along with that, the clinical data revealed that patients aged older possess high risk owing to high case fatality rate.

Moreover, investigation was done to identify the frequency of possible coinfection of SFTS and other zoonoses which possess similar clinical symptoms. SFTS is a zoonoses with high fatality rate that primarily infects human through tick bites. Furthermore, scrub typhus is a febrile illness transmit to humans via chigger mite. *H. longicornis* is the pivotal vector of SFTSV while *Leptotrombidium* spp. mites are the vectors of *O. tsutsugamushi* [84,85]. According to a previous study, SFTSV was found by RT-PCR in L. scutellare mite bites in China, suggesting that the mites may serve as a possible vector for the virus [84,85]. Till date, few cases of SFTS and scrub typhus co-infection have been reported. A study performed by Wi et al. also suggested that SFTSV and *O. tsutsugamushi* coinfection may occur in South Korea [85]. They reported 41%

coinfection prevalence and antibody titer was determined using commercial immunochromatography kit which is less sensitive and specific than other gold standard tests and require higher antigenic diversity among serotypes to determine the true positive results [85].

Also, involvement of different vectors in SFTS and scrub typhus portrayed that the actual prevalence of coinfection might be less than 41%. Following that, study performed by Yoo et al. reported mixed coinfection of SFTS and scrub typhus based on molecular analysis and observed the involvement of different vectors for both the diseases [86]. Though serological assay based on IFA is the gold standard for the detection of *O. tsutsugamushi*, it poses significant drawbacks in terms of requirement of paired sera, higher antigenic diversity among serotypes, and a standard antibody cutoff titer values to rule out the true prevalence rate in the endemic region [87]. Further, it is also challenging to eliminate the possibility of past or recent infection for cases which showing single high titer of scrub typhus antibody [87]. Therefore, to identify the true prevalence in a larger study population, I have performed a multicenter clinical cohort and systemically investigated the rate of coinfection of SFTS and scrub typhus based on molecular diagnostic methods. The seasonal distribution of the SFTS cases during 2015-2022 (up to September) projected the high prevalence rate during Autumn and fall season (June to October) which is very similar to the Korea Center for Disease Control and Prevention and the National Notifiable Disease Surveillance System reported overall prevalence pattern in South Korea during this time period (**Figure 4**) [88].

SFTS and scrub typhus poses similar clinical signs and symptoms, however SFTS has a greater fatality rate than scrub typhus [2]. Further, scrub typhus tends to present more subjective clinical manifestations than SFTS such as maculopapular skin rashes and eschar formation. As the skin rash or eschar in scrub typhus is distinct than the one in SFTS cases, this characteristic tends to poses important diagnostic value for experienced clinician [89,90]. Therefore, absence of eschar and skin rash poses great challenge in scrub typhus diagnosis. In our study, only one coinfected patient showed presence of maculopapular rash and eschar formation which makes the clinical differentiation of coinfection or single infection more difficult. Therefore, it is crucial to take SFTS into account in scrub typhus patients who may also have SFTSV infection [84].

The environmental transmission pattern and distribution of SFTSV and *O. tsutsugamushi* in indigenous nations like China, South Korea, and Japan must therefore be better understood. Moreover, it is necessary to conduct ongoing surveillance of SFTS patients, reporting in-depth clinical symptoms and related virus genotypes that are common in the region. Additionally, improved clinical procedures and outcomes are needed in areas where numerous tick- and mite-borne infections are common to elucidate concerns about the process of coinfection, such as whether it involves bites from various vectors or merely common vector. These areas call for more reliable differential diagnosis approaches as well as preventative and control measures.

Rickettsia infection usually manifests as fever, headache, and rash, as well as

muscle pain. The typical symptom is eschar-like skin lesions formed by the bite of a tick or mite, and the mortality rate is low under reasonable treatment. In our study, molecular diagnosis based on nested PCR was performed to identify 8 SFTS positive patients who were confirmed to have rickettsia species. The lack of rashes and eschar in the 8 patients in this study could be attributed to the skin lesions' invisibility and lack of discomfort, which made them challenging to spot and simple to ignore. RT-PCR or traditional PCR detection in diseased tissues can be used to diagnose rickettsial illnesses [91]. False negative results, however, could result from sampling errors, and patients with inconsequential skin lesions might be altogether disregarded. Due to similar clinical manifestations caused by different rickettsial infections, there are cross reactions in serological methods. Pathogen culture is difficult, and the application of molecular techniques in whole blood are limited so far. Thus, rapid and reliable molecular blood detection of rickettsial diseases is still difficult to achieve. Indirect immunofluorescence assay is considered to be the gold standard, but due to its extensive cross-reactivity, this method has limited use in the determination of species within serogroups [92]. In this study, I identified coinfection of *rickettsia monacensis* and *rickettsia tamurae* with SFTSV. Previously, few reports were published stating the incidence of spotted fever group rickettsia and SFTSV coinfection in Japan, northeast region of China but in our knowledge, this is the first study where I have identified the coinfection of rickettsia species with SFTSV in South Korea [93-94]. As a result, it is advised that when treating patients with SFTS, doctors should be aware of any rash or eschar symptoms, as well as

PCT and CRP levels. Additionally, individuals with SFTS who have a severe headache or whose symptoms have not significantly improved should use doxycycline as a preventative measure.

There is currently no vaccine or specific antiviral drug for SFTSV. Ribavirin is thought to be a possible antiviral agent for SFTS, but several retrospective studies have shown that ribavirin has not been effective in improving disease prognosis [95-96]. Li et al. reported that a calcium channel blocker benidipine hydrochloride can inhibit SFTSV infection by interfering with viral replication [97]. Additional research revealed that nifedipine can also prevented SFTSV infection but lack of proper clinical evidence regarding the same lead us to design new therapeutic molecule against SFTSV [97]. In our study, $EC_{50}$ values for all designed compounds were observed in the range between 100-200µg/mL which indicates that all the compounds are less potent owing to very weak antiviral activity. This could be because the solvent disposal for the solution, which was not done since this solutioning was done using the solvent dimethyl sulfoxide (DMSO), is quite difficult due to its high boiling point, resulted in a very trace amount of the active chemicals in the solution of DMSO (189°C). Although, I couldn't identify the potential therapeutic agents against SFTSV, I believe that more detailed investigation including thermodynamically stable water mapping analysis and combination therapy with other potential antivirals can be helpful to identify proper treatment options against SFTSV.

This study has certain limitations which I have mentioned here. Our findings related to

the genetic and phylogenetic analysis was solely based on the partial SFTSV gene sequences identified in our study. Thus, attention should be taken while extrapolating the evolutionary principles and molecular features of SFTSV in various contexts. It was widely anticipated that the proper epidemiological inquiry in accordance with the SFTSV epidemic features and the increased volume of analyzed genomic data would be of great assistance for a more thorough and understandable investigation of the molecular SFTSV epidemic mechanism. Further, there might be a selection bias due to the fact that, not all the scrub typhus and rickettsiosis confirmed patients further undergo SFTSV PCR because of unavailability of samples. Moreover, some patients' scrub typhus and rickettsiosis PCR tests may have yielded false-negative outcomes because they were conducted post doxycycline medication. In addition to that, I performed rickettsia nested PCR by targeting single partial gene sequence so further proper investigation needed to properly identify the true scenario. Therefore, considering this, it can be articulated that the true frequency of coinfection in individuals with suspected tick-borne infection will therefore be revealed by subsequent well-designed investigations using more detailed analysis on these diseases.

# VI. CONCLUSIONS

Overall, the genetic and epidemiological research on SFTSV deepens our knowledge of the genetic and pathogenic variety of SFTSV strains in South Korea. Along with that, the clinical data showed that individuals over the age of 60 have a high risk due to a high case fatality rate. Further, the virus propagation dynamics was understood which clearly indicates that SFTSV evolve in nature by reassortment, leading to the development of new genotypes. Moreover, our findings indicate that 1.6% and 6.2% of patients are coinfected with SFTS and scrub typhus and SFTS and rickettsiosis infection respectively. RT-PCR analysis for SFTSV using patients' whole blood samples showed high sensitivity but due to the relatively low bacterial loads in sera, efficient molecular detection for scrub typhus and rickettsiosis has some limits in typical clinical application. As a result, in regions where both diseases are common, empirical doxycycline treatment may be necessary until coinfection is eliminated and additional diagnostic tests for SFTS in scrub typhus and rickettsiosis patients are required. Furthermore, it is important to comprehend the environmental propagation characteristics and the regional distribution of SFTSV and other zoonoses in endemic nations like China, South Korea, and Japan. In addition, continuous surveillance studies and thorough investigation on SFTSV genome and SFTS propagation are necessary to make a positive contribution to preventing catastrophic SFTSV infection epidemics. I am optimistic that this research will help researchers properly understand the genomic structure and mutation of SFTSV and ignite general curiosity in the SFTS research.

# VII. REFERENCES

1. Zhang Y.Z., Zhou D.J., Qin X.C., Tian J.H., Xiong Y., Wang J.B., Chen X.P., Gao D.Y., He Y.W., Jin D., et al. The ecology, genetic diversity, and phylogeny of Huaiyangshan virus in China. J. Virol. 2012;86:2864–2868.
2. Yu X.J., Liang M.F., Zhang S.Y., Liu Y., Li J.D., Sun Y.L., Zhang L., Zhang Q.F., Popov V.L., Li C., et al. Fever with thrombocytopenia associated with a novel bunyavirus in China. New Engl. J. Med. 2011;364:1523–1532.
3. Xu B., Liu L., Huang X., Ma H., Zhang Y., Du Y., Wang P., Tang X., Wang H., Kang K., et al. Metagenomic analysis of fever, thrombocytopenia and leukopenia syndrome (FTLS) in Henan Province, China: Discovery of a new bunyavirus. PLoS Pathog. 2011;7:e1002369.
4. Walter C.T., Barr J.N. Recent advances in the molecular and cellular biology of bunyaviruses. J. Gen. Virol. 2011;92:2467–2484.
5. Fu Y., Li S., Zhang Z., Man S., Li X., Zhang W., Zhang C., Cheng X. Phylogeographic analysis of severe fever with thrombocytopenia syndrome virus from Zhoushan Islands, China: Implication for transmission across the ocean. Sci. Rep. 2016;6:19563.
6. Niu G., Li J., Liang M., Jiang X., Jiang M., Yin H., Wang Z., Li C., Zhang Q., Jin C., et al. Severe fever with thrombocytopenia syndrome virus among domesticated animals, China. Emerg. Infect. Dis. 2013;19:756–763.
7. Kim K.H., Yi J., Kim G., Choi S.J., Jun K.I., Kim N.H., Choe P.G., Kim N.J., Lee

J.K., Oh M.D. Severe fever with thrombocytopenia syndrome, South Korea, 2012. Emerg. Infect. Dis. 2013;19:1892–1894.

8. Takahashi T., Maeda K., Suzuki T., Ishido A., Shigeoka T., Tominaga T., Kamei T., Honda M., Ninomiya D., Sakai T., et al. The first identification and retrospective study of severe fever with thrombocytopenia syndrome in Japan. J. Infect. Dis. 2014;209:816–827.
9. Korea Disease Control and Prevention Agency Ticks and Rodents borne Infectious Diseases Guideline 2020. [(accessed on 6 January 2023)]; Available online: http://www.kdca.go.kr/board/board.es?mid=a20507020000&bid=0019&act=view&list_no=365644
10. M.S. Mehand, P. Millett, F. Al-Shorbaji, C. Roth, M.P. Kieny, B. Murgue World Health Organization methodology to prioritize emerging infectious diseases in need of research and development. Emerg Infect Dis, 24 (9) (2018), p. e171427
11. Liu Q., He B., Huang S.Y., Wei F., Zhu X.Q. Severe fever with thrombocytopenia syndrome, an emerging tick-borne zoonosis. Lancet Infect. Dis. 2014;14:763–772.
12. Kim U.J., Oh T.H., Kim B., Kim S.E., Kang S.J., Park K.H., Jung S.I., Jang H.C. Hyperferritinemia as a diagnostic marker for severe fever with thrombocytopenia syndrome. Dis. Markers. 2017;2017:6727184.
13. H. Li, Q.B. Lu, B. Xing, et al. Epidemiological and clinical features of laboratory-diagnosed severe fever with thrombocytopenia syndrome in China, 2011-17: a prospective observational study. Lancet Infect Dis, 18 (10) (2018), pp. 1127-1137.

14. Kim M.C., Chong Y.P., Lee S.O., Choi S.H., Kim Y.S., Woo J.H., Kim S.H. Differentiation of severe fever with thrombocytopenia syndrome from scrub typhus. Clin. Infect. Dis. 2018;66:1621–1624.
15. Miyamoto S., Ito T., Terada S., Eguchi T., Furubeppu H., Kawamura H., Yasuda T., Kakihana Y. Fulminant myocarditis associated with severe fever with thrombocytopenia syndrome: A case report. BMC Infect. Dis. 2019;19:266.
16. Sun Y., Liang M., Qu J., Jin C., Zhang Q., Li J., Jiang X., Wang Q., Lu J., Gu W., et al. Early diagnosis of novel SFTS bunyavirus infection by quantitative real-time RT-PCR assay. J. Clin. Virol. 2012;53:48–53.
17. Yoshikawa T., Fukushi S., Tani H., Fukuma A., Taniguchi S., Toda S., Shimazu Y., Yano K., Morimitsu T., Ando K., et al. Sensitive and specific PCR systems for detection of both Chinese and Japanese severe fever with thrombocytopenia syndrome virus strains and prediction of patient survival based on viral load. J. Clin. Microbiol. 2014;52:3325–3333.
18. Huang X.Y., Hu X.N., Ma H., Du Y.H., Ma H.X., Kang K., You A.G., Wang H.F., Zhang L., Chen H.M., et al. Detection of new bunyavirus RNA by reverse transcription-loop-mediated isothermal amplification. J. Clin. Microbiol. 2014;52:531–535.
19. Baek Y.H., Cheon H.S., Park S.J., Lloren K.K.S., Ahn S.J., Jeong J.H., Choi W.S., Yu M.A., Kwon H.I., Kwon J.J., et al. Simple, rapid and sensitive portable molecular diagnosis of SFTS virus using reverse transcriptional loop-mediated isothermal

amplification (RT-LAMP) J. Microbiol. Biotechnol. 2018;28:1928–1936.

20. Ra S.H., Kim M.J., Kim M.C., Park S.Y., Park S.Y., Chong Y.P., Lee S.O., Choi S.H., Kim Y.S., Lee K.H., et al. Kinetics of serological response in patients with severe fever with thrombocytopenia syndrome. Viruses. 2020;13:6.
21. He F, Zheng X, Zhang Z. Clinical features of severe fever with thrombocytopenia syndrome and analysis of risk factors for mortality. BMC Infect Dis. 2021; 14;21(1):1253.
22. Y. Kobayashi, H. Kato, T. Yamagishi, et al. Severe fever with thrombocytopenia syndrome, Japan, 2013-2017. Emerg Infect Dis, 26 (4) (2020), pp. 692-699
23. Z. He, B. Wang, Y. Li, et al. Severe fever with thrombocytopenia syndrome: a systematic review and meta-analysis of epidemiology, clinical signs, routine laboratory diagnosis, risk factors, and outcomes. BMC Infect Dis, 20 (1) (2020), p. 575
24. X.J. Yu, M.F. Liang, S.Y. Zhang, et al. Fever with thrombocytopenia associated with a novel bunyavirus in China. N Engl J Med, 364 (16) (2011), pp. 1523-1532
25. K.H. Kim, J. Yi, G. Kim, et al. Severe fever with thrombocytopenia syndrome, South Korea, 2012. Emerg Infect Dis, 19 (11) (2013), pp. 1892-1894
26. T. Takahashi, K. Maeda, T. Suzuki, et al. The first identification and retrospective study of severe fever with thrombocytopenia syndrome in Japan. J Infect Dis, 209 (6) (2014), pp. 816-827
27. X.C. Tran, Y. Yun, L. Van An, et al. Endemic severe fever with thrombocytopenia

syndrome, Vietnam. Emerg Infect Dis, 25 (5) (2019), pp. 1029-1031

28. A.M. Win, Y.T.H. Nguyen, Y. Kim, et al. Genotypic heterogeneity of orientia tsutsugamushi in scrub typhus. patients and thrombocytopenia syndrome co-infection, Myanmar. Emerg Infect Dis, 26 (8) (2020), pp. 1878-1881
29. C. Daengnoi, S. Ongkittikul, R. Watanawong, P. Rompho. Severe fever with thrombocytopenia syndrome virus: the first case report in Thailand Bangkok Med J, 16 (2) (2020), pp. 204-206
30. Peng S.H., Yang S.L., Tang S.E., Wang T.C., Hsu T.C., Su C.L., Chen M.Y., Shimojima M., Yoshikawa T., Shu P.Y. Human case of severe fever with thrombocytopenia syndrome virus infection, Taiwan, 2019. Emerg. Infect. Dis. 2020;26:1612–1614.
31. Zohaib A., Zhang J., Saqib M., Athar M.A., Hussain M.H., Chen J., Sial A.U., Tayyab M.H., Batool M., Khan S., et al. Serologic evidence of severe fever with thrombocytopenia syndrome virus and related viruses in Pakistan. Emerg. Infect. Dis. 2020;26:1513–1516.
32. McMullan L.K., Folk S.M., Kelly A.J., MacNeil A., Goldsmith C.S., Metcalfe M.G., Batten B.C., Albariño C.G., Zaki S.R., Rollin P.E., et al. A new phlebovirus associated with severe febrile illness in Missouri. New Engl. J. Med. 2012;367:834–841.
33. Staples J.E., Pastula D.M., Panella A.J., Rabe I.B., Kosoy O.I., Walker W.L., Velez J.O., Lambert A.J., Fischer M. Investigation of heartland virus disease throughout

the United States, 2013–2017. Open Forum Infect. Dis. 2020;7:ofaa125.

34. Li J., Li S., Yang L., Cao P., Lu J. Severe fever with thrombocytopenia syndrome virus: A highly lethal bunyavirus. Crit. Rev. Microbiol. 2021;47:112–125.
35. Yoo J.R., Heo S.T., Song S.W., Bae S.G., Lee S., Choi S., Lee C., Jeong S., Kim M., Sa W., et al. Severe fever with thrombocytopenia syndrome virus in ticks and sfts incidence in humans, South Korea. Emerg. Infect. Dis. 2020;26:2292–2294.
36. Hoogstraal H., Roberts F.H., Kohls G.M., Tipton V.J. Review of Haemaphysalis (kaiseriana) Longicornis neumann (resurrected) of Australia, New Zealand, New Caledonia, Fiji, Japan, Korea, and Northeastern China and USSR, and its parthenogenetic and bisexual populations (Ixodoidea, Ixodidae) J. Parasitol. 1968;54:1197–1213.
37. Kim U.J., Kim D.M., Kim S.E., Kang S.J., Jang H.C., Park K.H., Jung S.I. Case report: Detection of the identical virus in a patient presenting with severe fever with thrombocytopenia syndrome encephalopathy and the tick that bit her. BMC Infect. Dis. 2018;18:181.
38. Zhuang L., Sun Y., Cui X.M., Tang F., Hu J.G., Wang L.Y., Cui N., Yang Z.D., Huang D.D., Zhang X.A., et al. Transmission of severe fever with thrombocytopenia syndrome virus by haemaphysalis longicornis ticks, China. Emerg. Infect. Dis. 2018;24:868–871.
39. Sun Y., Jin C., Zhan F., Wang X., Liang M., Zhang Q., Ding S., Guan X., Huo X., Li C., et al. Host cytokine storm is associated with disease severity of severe fever

with thrombocytopenia syndrome. J. Infect. Dis. 2012;206:1085–1094.

40. Hu L.F., Wu T., Wang B., Wei Y.Y., Kong Q.X., Ye Y., Yin H.F., Li J.B. The regulation of seventeen inflammatory mediators are associated with patient outcomes in severe fever with thrombocytopenia syndrome. Sci. Rep. 2018;8:159.
41. J.W. Seo, D. Kim, N. Yun, D.M. Kim. Clinical update of severe fever with thrombocytopenia syndrome. Viruses, 13 (7) (2021), p. 1213.
42. Kida K., Matsuoka Y., Shimoda T., Matsuoka H., Yamada H., Saito T., Imataki O., Kadowaki N., Noguchi K., Maeda K., et al. A case of cat-to-human transmission of severe fever with thrombocytopenia syndrome virus. Jpn. J. Infect. Dis. 2019;72:356–358.
43. Park E.S., Shimojima M., Nagata N., Ami Y., Yoshikawa T., Iwata-Yoshikawa N., Fukushi S., Watanabe S., Kurosu T., Kataoka M., et al. Severe fever with thrombocytopenia syndrome phlebovirus causes lethal viral hemorrhagic fever in cats. Sci. Rep. 2019;9:11990.
44. Ryu B.H., Kim J.Y., Kim T., Kim M.C., Kim M.J., Chong Y.P., Lee S.O., Choi S.H., Kim Y.S., Woo J.H., et al. Extensive severe fever with thrombocytopenia syndrome virus contamination in surrounding environment in patient rooms. Clin. Microbiol. Infect. 2018;24:911.e1–911.e4.
45. Kim CM, Kim DM, Yun NR. Clinical Usefulness of Nested Reverse-Transcription Polymerase Chain Reaction for the Diagnosis of Severe Fever with Thrombocytopenia Syndrome. Am J Trop Med Hyg. 2021 Aug 2;105(4):999-1003.

46. Hwang J, Kang JG, Oh SS, et al. Molecular detection of severe fever with thrombocytopenia syndrome virus (SFTSV) in feral cats from Seoul, Korea. Ticks Tick Borne Dis. 2017;8(1):9–12.

47. Jun H, Jegal S, Kim-Jeon MD, Roh JY, Lee WG, Park SH, Ahn SK, Lee J, Gong YW, Kwon MJ, Bahk YY, Kim TS. Three-year surveillance (2016–2018) of chigger mite vector for tsutsugamushi disease in the Hwaseong-Si area of Gyeonggi-Do Republic of Korea. Entomol Res 2020;50: 63-73

48. Bahk YY, Jun H, Park SH, Jung H, Jegal S, Kim-Jeon MD, Roh JY, Lee WG, Ahn SK, Lee J, Joo K, Gong YW, Kwon MJ, Kim TS. Surveillance of chigger mite vectors for tsutsugamushi disease in the Hwaseong Area, Gyeonggi-do, Republic of Korea, 2015. Korean J Parasitol 2020;58: 301-308

49. Chatterjee, S., Kim, CM. & Kim, DM. Potential efficacy of existing drug molecules against severe fever with thrombocytopenia syndrome virus: an in silico study. Sci Rep 11, 20857 (2021).

50. Zhou, H. et al. Te nucleoprotein of severe fever with thrombocytopenia syndrome virus processes a stable hexameric ring to facilitate RNA encapsidation. Prot. Cell 4, 445–455 (2013).

51. Olschewski, S., Cusack, S. & Rosenthal, M. Te Cap-Snatching Mechanism of Bunyaviruses. Trends Microbiol. 28, 293–303 (2020).

52. Joshi, A., Sunil Krishnan, G. & Kaushik, V. Molecular docking and simulation investigation: effect of beta-sesquiphellandrene with ionic integration on SARS-

CoV2 and SFTS viruses. J. Genet. Eng. Biotechnol. 18, 78 (2020).

53. Laskowski, R. A., Jabłońska, J., Pravda, L., Vařeková, R. S. & Tornton, J. M. PDBsum: Structural summaries of PDB entries. Prot.Sci. 27(1), 129–134 (2018).
54. Morris, G. M. et al. AutoDock4 and AutoDockTools4: Automated docking with selective receptor flexibility. J. Comput. Chem.30(16), 2785–2791 (2009).
55. O'Boyle, N. M. et al. Open Babel: An open chemical toolbox. J. Cheminform. 7(3), 33 (2011).
56. Chen, C., Huang, Y., Ji, X. & Xiao, Y. Efficiently finding the minimum free energy path from steepest descent path. J. Chem. Phys.138(16), 1622 (2013).
57. Trott, O. & Olson, A. J. AutoDock Vina: improving the speed and accuracy of docking with a new scoring function, efficient optimization, and multithreading. J. Comput. Chem. 31(2), 455–461 (2010).
58. Sen, D., Debnath, P., Debnath, B., Bhaumik, S. & Debnath, S. Identification of potential inhibitors of SARS-CoV-2 main protease and spike receptor from 10 important spices through structure-based virtual screening and molecular dynamic study. J. Biomol. Struct. Dyn. 1, 1–22 (2020).
59. Abraham, M. J. et al. GROMACS: High performance molecular simulations through multi-level parallelism from laptops to supercomputers. SofwareX 1, 19–25 (2015).
60. Huang, J. & MacKerell, A. D. Jr. CHARMM36 all-atom additive protein force feld: validation based on comparison to NMR data. J. Comput. Chem. 34(25), 2135–2145 (2013).

61. Zoete, V., Cuendet, M. A., Grosdidier, A. & Michielin, O. SwissParam: A fast force field generation tool for small organic molecules. J Comput Chem. 32(11), 2359–2368 (2011).

62. Jorgensen, W. L., Chandrasekhar, J., Madura, J. D., Impey, R. W. & Klein, M. L. Comparison of simple potential functions for simulating liquid water. J. Chem. Phys. 79(2), 926–935 (1983).

63. Gupta, M. K. et al. Insights into the structure-function relationship of brown plant hopper resistance protein, Bph14 of rice plant: a computational structural biology approach. J. Biomol. Struct. Dyn. 37(7), 1649–1665 (2019).

64. Huang, Y., Chen, W., Wallace, J. A. & Shen, J. All-atom continuous constant pH molecular dynamics with particle mesh ewald and titratable water. J. Chem. Teory Comput. 12(11), 5411–5421 (2016).

65. Parrinello, M. & Rahman, A. Polymorphic transitions in single crystals: A new molecular dynamics method. J. Appl. Phys. 52, 7182–7190 (1981).

66. Kufareva, I. & Abagyan, R. Methods of protein structure comparison. Methods Mol Biol. 857, 231–257 (2012).

67. Martínez, L. Automatic identification of mobile and rigid substructures in molecular dynamics simulations and fractional structural fluctuation analysis. PLoS ONE 10(3), e0119264 (2015).

68. Lobanov, MIu., Bogatyreva, N. S. & Galzitskaia, O. V. Radius of gyration is indicator of compactness of protein structure. Mol.Biol. (Mosk) 42(4), 701–706

(2008).

69. Yun SM, et al. Molecular genomic characterization of tick- and human-derived severe fever with thrombocytopenia syndrome virus isolates from South Korea. PLoS Negl Trop Dis. 2017;11(9):e0005893.
70. Huang, H. & Simmerling, C. Fast pairwise approximation of solvent accessible surface area for implicit solvent simulations of proteins on CPUs and GPUs. J. Chem. Theory Comput. 14(11), 5797–5814 (2018).
71. Humphrey, W., Dalke, A. & Schulten, K. VMD: visual molecular dynamics. J Mol Graph 14(1), 33–8 (1996).
72. M. Shimojima, S. Fukushi, H. Tani, T. Yoshikawa, S. Morikawa, M. Saijo Severe fever with thrombocytopenia syndrome in Japan Uirusu, 63 (2013), pp. 7-12.
73. K.-H. Kim, J. Yi, G. Kim, S.J. Choi, K.I. Jun, N.-H. Kim, P.G. Choe, N.-J. Kim, J.-K. Lee, M.-d. Oh. Severe fever with thrombocytopenia syndrome, South Korea, 2012. Emerg. Infect. Dis., 19 (2013), pp. 1892-1894
74. L.K. McMullan, S.M. Folk, A.J. Kelly, A. MacNeil, C.S. Goldsmith, M.G. Metcalfe, B.C. Batten, C.G. Albariño, S.R. Zaki, P.E. Rollin. A new phlebovirus associated with severe febrile illness in Missouri. N. Engl. J. Med., 367 (2012), pp. 834-841,
75. J. Wang, P. Selleck, M. Yu, W. Ha, C. Rootes, R. Gales, T. Wise, S. Crameri, H. Chen, I. Broz Novel phlebovirus with zoonotic potential isolated from ticks, Australia. Emerg. Infect. Dis., 20 (2014), p. 1040, 10.3201/eid2006.140003
76. D. Mourya, P. Yadav, A. Basu, A. Shete, D. Patil, D. Zawar, T. Majumdar, P.

Kokate, P. Sarkale, C. Raut, Malsoor virus, a novel bat phlebovirus, is closely related to severe fever with thrombocytopenia syndrome virus and heartland virus. J. Virol., 88 (2014), pp. 3605-3609.

77. Sun J, Lu L, Wu H, Yang J, Ren J, Liu Q. The changing epidemiological characteristics of severe fever with thrombocytopenia syndrome in China, 2011-2016. Sci Rep. 2017;7(1):9236
78. Shi J, et al. Migration, recombination, and reassortment are involved in the evolution of severe fever with thrombocytopenia syndrome bunyavirus. Infect Genet Evol. 2017;47:109–117.
79. Li Z, et al. Increased prevalence of severe fever with thrombocytopenia syndrome in Eastern China clustered with multiple genotypes and reasserted virus during 2010-2015. Sci Rep. 2017;7(1):6503.
80. Zhan J, et al. Current status of severe fever with thrombocytopenia syndrome in China. Virol Sin. 2017;32(1):51–62
81. Gokuden M, et al. Low seroprevalence of severe fever with thrombocytopenia syndrome virus antibodies in individuals living in an endemic area in Japan. Jpn J Infect Dis. 2018;71(3):225–228.
82. Severe fever thrombocytopenia syndrome (SFTS). Information of infectious diseases. Tokyo: National Institute of Infectious Diseases. https://www.niid.go.jp/niid/ja/diseases/sa/sfts.html. Accessed December 16, 2019.
83. Robles NJC, Han HJ, Park SJ, Choi YK. Epidemiology of severe fever and

thrombocytopenia syndrome virus infection and the need for therapeutics for the prevention. Clin Exp Vaccine Res. 2018;7(1):43–50.

84. Wi YM, Woo HI, Park D, Lee KH, Kang CI, Chung DR, Peck KR, Song JH, 2016. Severe fever with thrombocytopenia syndrome in patients suspected of having scrub typhus. Emerg Infect Dis 22: 1992–1995.
85. Weitzel T, Dittrich S, L ´opez J, Phuklia W, Martinez-Valdebenito C, Vel ´asquez K, Blacksell SD, Paris DH, Abarca K, 2016. Endemic scrub typhus in South America. N Engl J Med 375: 954–961.
86. Yoo JR, Heo ST, Park D, Kim H, Fukuma A, Fukushi S, Shimojima M, Lee KH, 2016. Family cluster analysis of severe fever with thrombocytopenia syndrome virus infection in Korea. Am J Trop Med Hyg 95: 1351–1357.
87. Ericsson CD, Jensenius M, Fournier P-E, Raoult D (2004) Rickettsioses and the international traveler. Clin Infect Dis 39:1493–1499.
88. https://www.kdca.go.kr/npt/biz/npp/ist/simple/simplePdStatsMain.do#
89. Lee CS, Hwang JH. Images in clinical medicine. Scrub typhus. N Engl J Med. 2015;373(25):2455.
90. Liu YX, Feng D, Suo JJ, Xing YB, Liu G, Liu LH, et al. Clinical characteristics of the autumn-winter type scrub typhus cases in south of Shandong province, northern China. BMC Infect Dis. 2009;9:82.
91. Denison AM, Amin BD, Nicholson WL, Paddock CD. Detection of Rickettsia rickettsii, Rickettsia parkeri, and Rickettsia akari in skin biopsy specimens using a

multiplex real-time polymerase chain reaction assay. Clin Infect Dis. 2014 Sep 1;59(5):635-42.

92. Paris DH, Dumler JS. State of the art of diagnosis of rickettsial diseases: the use of blood specimens for diagnosis of scrub typhus, spotted fever group rickettsiosis, and murine typhus. Curr Opin Infect Dis. 2016 Oct;29(5):433-9
93. Fujikawa T, Yoshikawa T, Kurosu T, Shimojima M, Saijo M, Yokota K. Co-infection with Severe Fever with Thrombocytopenia Syndrome Virus and Rickettsia japonica after Tick Bite, Japan. Emerg Infect Dis. 2021 Apr;27(4):1247-1249
94. Yue Ma, Hongyan Liu, Jixu Li, et al. Coinfection of SFTSV Genotype A with Rickettsia among Farmers in Northeast. Authorea. September 21, 2020.
95. Li, H. et al. Epidemiological and clinical features of laboratory-diagnosed severe fever with thrombocytopenia syndrome in China, 2011-17: a prospective observational study. Lancet Infect. Dis. 18, 1127–1137 (2018)
96. Wei Liu, Qing-Bin Lu, Ning Cui, et al. Case-Fatality Ratio and Effectiveness of Ribavirin Therapy Among Hospitalized Patients in China Who Had Severe Fever With Thrombocytopenia Syndrome, Clinical Infectious Diseases, Volume 57, Issue 9, 1 November 2013, Pages 1292–1299.
97. Li H., Zhang L. K., Li S. F., Zhang S. F., Wan W. W., Zhang Y. L., et al. (2019). Calcium channel blockers reduce severe fever with thrombocytopenia syndrome virus (SFTSV) related fatality. Cell Res. 29, 739–753.

# VIII. ACKNOWLEDGEMENTS

I would like to express my sincere gratitude to my advisor **Prof. Dong-Min Kim** for his guidance and motivation. I can't thank him enough for providing me the great opportunity to pursue my Ph.D. under his supervision. I'm grateful for his continuous support, patience and sharing of his immense research knowledge and ideas with me. His great influence and support in professional as well as personal life shaped me who I am today. Without his guidance and constant feedback, this Ph.D. would not have been possible.

I would like to express my sincere thankfulness to **Prof. Choon-Mee Kim** for providing experimental guidance and support throughout this research period.

My sincere thanks to all of my thesis committee members for reviewing my thesis and providing their able guidance to improve my work.

I cannot thank enough to my beautiful mother, **Mrs. Chaitali Chatterjee** for her enormous sacrifice and constant support towards me to achieve my goals. Her love and guidance throughout my journey always empower me to overcome all the hurdles of my life. Without her I couldn't even think of pursuing my higher studies in South Korea, far away from my home.

I would like to extend my tribute to my heavenly father, **Mr. Nimai Chatterjee** who is no more to see his daughter's success physically, but his heavenly blessings, love, and deep understanding of life ease my path towards success.

I am also grateful to my university members for having me as a doctoral student and helping me to pursue my dream.

I would like to sincerely thank my colleagues and lab members for their immense support, feedback, cooperation and of course friendship.

Last but not the least, I would acknowledge my love to my beloved partner for always motivating me and supporting me through thick and thin and helping me to achieve my dream.

*To my dearest*

*Mom, Dad, and my beloved partner*

*who always picked me up on time*

*and*

*encouraged me to go on every adventure,*

*especially this one*

*thank you*